ACTA TECNOLOGÍA

electronic journal
ISSN 2453-675X
Volume 10
Issue 3
2024

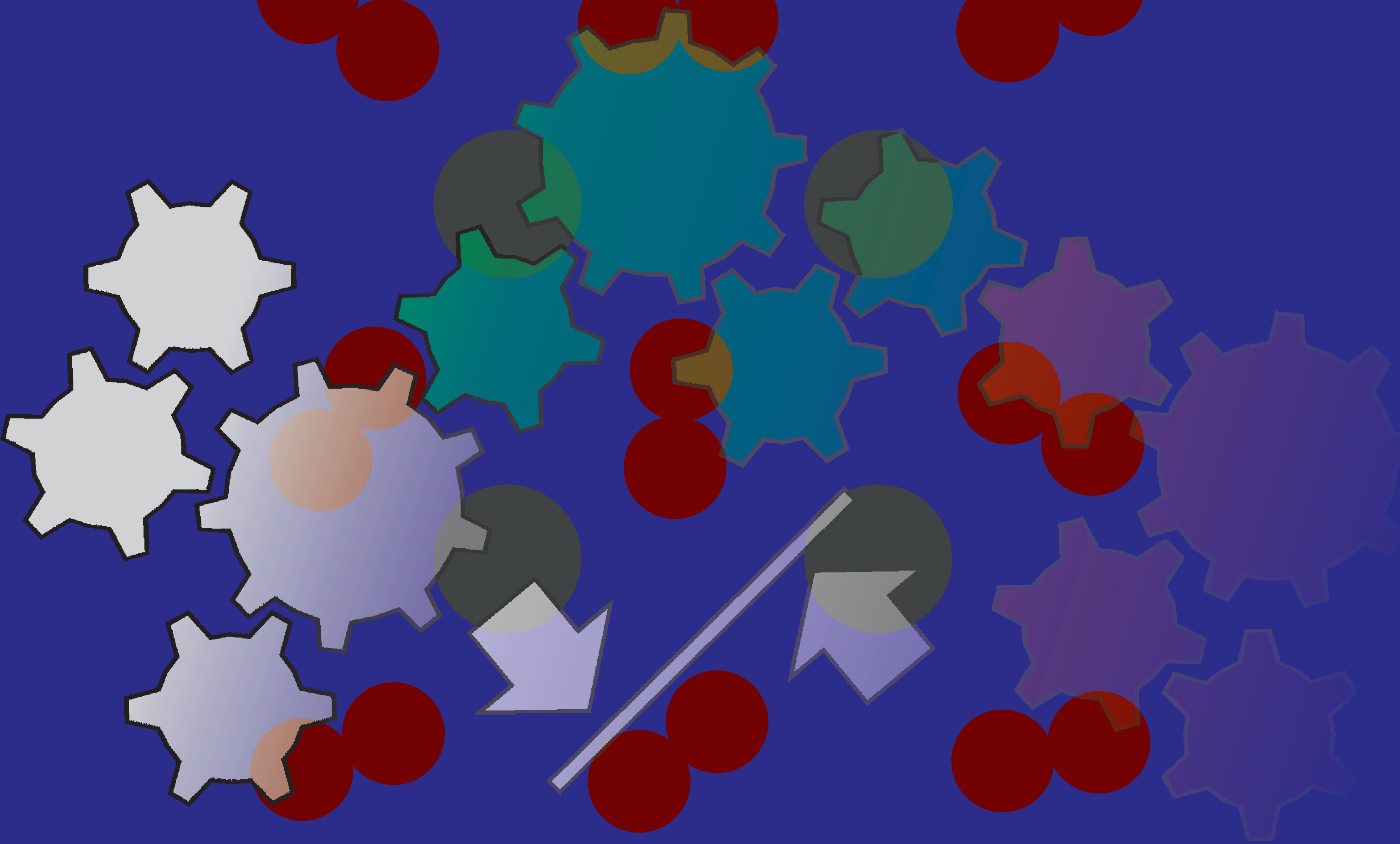

International Scientific Journal about Technologies

CONTENTS

(SEPTEMBER 2024)

Acta Tecnología - International Scientific Journal about Technologies
Volume: 10 2024 Issue: 3 Pages: 81-86 ISSN 2453-675X

https://doi.org/10.22306/atec.v10i3.205 *Received: 18 June 2024; Revised: 31 Aug. 2024; Accepted: 12 Sep. 2024*

Extracellular matrix decellularization approaches for 3D tissue printing

Jana Cajkova
Faculty of Mechanical Engineering, Technical University of Kosice, Department of Biomedical Engineering and Measurement, Letná 1/9, 042 00 Košice, Slovak Republic, EU,
jana.cajkova@tuke.sk (corresponding author)
Marianna Trebunova
Faculty of Mechanical Engineering, Technical University of Kosice, Department of Biomedical Engineering and Measurement, Letná 1/9, 042 00 Košice, Slovak Republic, EU,
marianna.trebunova@tuke.sk
Darina Bacenkova
Faculty of Mechanical Engineering, Technical University of Kosice, Department of Biomedical Engineering and Measurement, Letná 1/9, 042 00 Košice, Slovak Republic, EU,
darina.bacenkova@tuke.sk

Keywords: 3D bioprinting, extracellular matrix, bioink, regenerative medicine.
Abstract: 3D bioprinting holds transformative potential for the field of regenerative medicine, offering unprecedented opportunities for the fabrication of complex, living tissues. Central to this technological innovation is the development of suitable bioinks that can accurately replicate the native cellular environment. Decellularized extracellular matrix (dECM) has emerged as a promising candidate due to its inherent biocompatibility, bioactivity, and structural resemblance to native tissues. Decellularization is a crucial process in tissue engineering that involves the removal of cellular components from the extracellular matrix (ECM) to create scaffolds suitable for tissue regeneration. This article provides a review of some decellularization methods, categorizing them into physical, chemical, and biological approaches. The article discusses the advantages and limitations of each method, highlighting the need to balance effective decellularization with the preservation of the ECM's functional properties. Understanding these methods is critical for developing optimized scaffolds for various tissue engineering applications.

1 Introduction

The field of tissue engineering and regenerative medicine is witnessing a revolution with the advent of 3D bioprinting technology, which allows for the precise construction of complex tissue structures layer by layer. A critical component of this technology is the bioink, a substance composed of living cells and biomaterials that can be printed into tissue-like structures. Among various bioink options, decellularized extracellular matrix (dECM) is emerging as a highly promising candidate due to its unique biochemical and mechanical properties. Derived from natural tissues, dECM retains the intricate composition of proteins, growth factors, and structural molecules, providing an optimal environment for cell growth and differentiation. This article explores the potential of dECM as a bioink in 3D printing, examining its advantages, challenges, and the latest advancements in its application for fabricating functional living tissues. By leveraging the inherent biological cues of dECM, researchers aim to create more physiologically relevant tissue constructs, advancing the frontier of personalized medicine and organ transplantation [1,2]. However, the process of decellularization, which involves removing cellular components from the ECM while preserving its structure and function, is a delicate and complex task. Different decellularization techniques, physical, chemical, and biological, offer unique advantages and challenges that influence the quality and efficacy of the resulting dECM. The choice of method can significantly impact the mechanical properties, biocompatibility, and bioactivity of the dECM, thereby affecting the success of the bioprinted tissue [3,4].

2 Extracellular matrix

There is no tissue in the body that consist of homogenous compositions of its extracellular matrix (ECM), cell phenotype, and mechanical characteristics. Extracellular matrix and its constituents influence the survival, self-renewal, and proliferation of the cells. The mechanical properties and the composition of ECM play critical roles in fate of the stem cell [1]. The ECM comprises a diverse array of macromolecules whose specific composition and structural organization vary among different tissues. The primary components of ECMs include fibrous-forming proteins such as collagens, elastin, fibronectin (FN), laminins, glycoproteins, proteoglycans (PGs), and glycosaminoglycans (GAGs), the latter of which are characterized by their high acidity and hydration levels. In most tissues, the predominant constituents of ECMs are fibril-forming collagen type I, while in cartilage, collagen type II is most prevalent. These collagen types are associated with other collagen forms, ECM proteins, and

PGs, forming extensive fibrillar structures. These multimolecular assemblies are interlinked with ECM molecules, which further interact with one another, thereby constructing the complex three-dimensional matrix network (Figure 1) [2].
Mammalian tissue is comprised of more than 300 ECM proteins and multiple ECM-modifying enzymes, ECM-binding growth factors, and other ECM-associated proteins that mediate structural, mechanical, biophysical, and biochemical cues to cells (Table 1) [3].

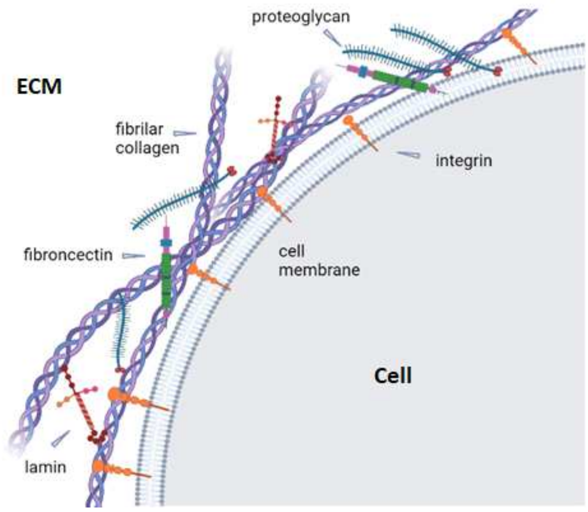

Figure 1 Illustration of composition of extracellular matrix (ECM), showing cellular engagement with biomolecules and primary components of ECM (created with Biorender.com)

The integrins are a family of α, β heterodimeric receptors that mediate dynamic linkages between extracellular adhesion molecules and the intracellular actin cytoskeleton [4]. Proteoglycans are complex glycoconjugates that contain one or more glycosaminoglycan chains, such as chondroitin sulfate, heparan sulfate, or keratan sulfate, covalently bound to a protein. Fibronectin mediates a wide variety of cellular interactions with the extracellular matrix (ECM) and plays important roles in cell adhesion, migration, growth, and differentiation. The lamins are the major architectural proteins of the animal cell nucleus and ensure mechanical stability of the nuclear membrane [5].

One of the significant roles of ECM is the provision of 3D structural support as a substrate in cellular migration and as a transmitter of biomechanical forces [6]. The mechanisms by which ECM offers these activities are varied. The transmission of mechanical cues is provided by: (a) signalling through direct cellular binding; (b) through the sequestration and regulation of soluble growth factors and cytokines. Therefore, ECM can be considered a highly specialized substrate for both mechanical support and functional substrate for cell growth and signalling. The components of ECM also provide spatial separation between specialized sections of tissue, such as the basement membrane separating the mucosal lining of the intestine from the submucosal tissue. The extracellular matrix also mediates the stress processes and regulates cell proliferation and phenotype expression based on the current state of the cell and tissue [11]. The key to the cell signalling is an interaction between ECM proteins and integrins, which are heterodimeric transmembrane receptors. Integrins bind to the ECM protein as their ligands, therefore they can respond to any mechanical or biochemical change in ECM [6] [7]

Table 1 Components of extracellular matrix (ECM) with brief description of their functions [3,8,9,10]

<table>
<tr><th>ECM</th><th colspan="2">Activity</th></tr>
<tr><td>Collagen</td><td colspan="2">dictates the tissue architecture, shape, and organization</td></tr>
<tr><td rowspan="8">Proteoglycans</td><td>Decorin</td><td rowspan="2">regulate collagen fibril assembly</td></tr>
<tr><td>Lumican</td></tr>
<tr><td rowspan="3">Aggrecan</td><td>causes elasticity and high biomechanical resistance</td></tr>
<tr><td>binds hyaluronan – facilitating of chondrocyte-chondrocyte and chondrocyte-matrix interactions</td></tr>
<tr><td>arranges the extracellular areas between neurons in the brain</td></tr>
<tr><td>Versican</td><td>modulates cell adhesion, migration, proliferation</td></tr>
<tr><td>Neurocan</td><td>modulates cell adhesion and migration</td></tr>
<tr><td>Brevican</td><td>may play a role in maintaining the extracellular environment of mature brain</td></tr>
<tr><td rowspan="2">Lamins</td><td colspan="2">create network between cells and receptors on cell surface</td></tr>
<tr><td colspan="2">essential for early embryonic development and organogenesis</td></tr>
<tr><td>Fibronectin</td><td colspan="2">provides attachment and migration of cells, growth, differentiation</td></tr>
<tr><td>Elastin</td><td colspan="2">provides elasticity to the tissue</td></tr>
</table>

3 Decellularised extracellular matrix

As there is no singular ideal approach for decellularization, the protocol must be customized according to the source of the tissue. Same decellularization process can bring different results in different tissues [11]. For the successful preparation of dECM without any adverse host reaction, it is necessary to remove cells from tissues while preserving the native ECM components and structure (Figure 2). Any residual cell material is responsible for the induction of an inflammatory response and subsequently an immune reaction [12]. The immune response is tightly connected with any DNA residues, as the host recognizes any unfamiliar genetic material and evaluates it as a threat, therefore, starting the processes of the immune system to eliminate it [13]. However, at the moment, it is not possible to reliably remove all the genetic information from the ECM in the process of decellularization. Therefore, there are three criteria established to describe dECM: 1) maximum of 50 µg residual double-stranded DNA per mg of ECM dry weight, 2) DNA fragments smaller than 200 base pair, and 3) 4', 6-diamidino-2-phenylindole (DAPI) or hematoxylin and eosin (H&E) staining proving lack of visible nuclear material [1,9,14].

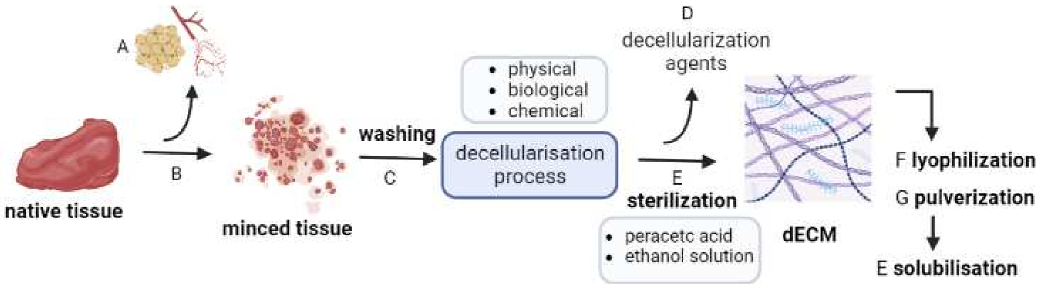

Figure 2 Process of preparation of dECM (Created with Biorender.com)

There are various techniques for decellularization, such as physical, enzymatic, chemical, or their combination (Table 2). The decellularization can alter the composition of ECM therefore it is essential to select a fitting mechanism to maintain the wanted structure It is crucial to mention that any of the chosen methods disrupt the composition of ECM on some level therefore the goal is to minimize the harmful effects [15]. It is also important to note, that each tissue requires a specific approach to achieve successful decellularization with ECM properties preserved [16].

3.1 *Physical decellularization*

Physical ways of removing cellular material from tissues work by breaking cell membranes and producing unfavourable cellular conditions that can induce apoptosis [13]. Lack of chemicals used in physical processing and the benefit of being consistent throughout tissue makes physical decellularization a common method between researchers. Furthermore, effects of the process are more predictable than those of chemical or enzymatic decellularizing agents. However, physical treatment alone is frequently insufficient for decellularization [15]. While it can cause cell lysis, it is unsuccessful at totally eliminating cell or nuclear remains. Nonetheless, it can be utilized in tandem with chemical, biological, or enzymatic decellularizing agents to reduce exposure times and enhance ECM proteomic content retention [17].

One of the earliest physical processes to achieve decellularization is cyclic freeze-thaw method. It is cost-effective process to prepare dECM. However, recent studies show, that extensive cyclic freeze-thaw decellularization can cause and immune response and impact the biochemical abilities of dECM, as the microstructure of a collagen at molecular level could be gradually altered by ice creation several cycles in [19]. Pu Luo et al. prepared dECM through repeated freeze-thaw cycles with combination with other methods to design an efficient decellularization method. Extracellular matrix was obtained from porcine peritoneum, underwent n = 0 (control) 3 and 7 freeze thaw cycles and then the decellularization continued with alkaline and acids, organic solvents, and hypotonic/hypertonic solutions.

Table 2 Summary of methods used in decellularization of extracellular matrix with their advantages and disadvantages

Method	Procedure	Pros	Cons
Physical	Freeze-thaw cycle	tissue integrity	relatively high DNA content left
		preserved elastic modulus	alteration of collagen fibrils
	Ultrasonic waves	whole cell removal	uncontrolled cavitation
			destructive effects on retinal tissue
	Hydrostatic pressure method	collagen well preserved	addition of chemical agents to remove DNA residues
	Electroporat-ion	preservation of ECM - neighboring tissue	limited size of the decellularized tissue
Chemical	Acids and bases	sterilization capabilities	insufficient cell removal
		separation of cellular components	alters mechanical properties
	Triton X-100	removal of cellular residues from thin tissue	elastin decrease
		myosin and actin preserved	effectivity varies between tissues
	SDSc	effective in dense tissues	damage of collagen
			removing growth factors
Biological	Trypsin	does not affect the amount of collagen	prolonged exposure removes disrupts ECM
		effective cell removal	removes laminin, fibronectin elastin
	Endo/Exo-nucleases	hydrolysis of the terminal bonds of RNA and DNA	difficult to remove from the tissue
			invokes an immune response

The resulted mass was subsequently lyophilised and sterilised as per standard procedure. As typical temperatures for freeze-thaw cycle are - 20° C and - 80° C, it takes a lot of time to remove the cell material thoroughly, however in this study, the liquid nitrogen was used to freeze the tissue for 5 minutes and then thawed at the room temperature. Subsequent analysis with histological staining confirmed no visible nuclei. Surface morphology and pore size of the dECM structure were characterized to analyse the impact of freeze-thaw cycles (FTC). SEM images showed a decrease in average pore size from 10 mm to 5 mm after 7 FTC and collagen diameter was half the size of that in the control group. Mercury intrusion porosimetry (MIP) and atomic force microscopy (AFM) confirmed the theory that the pore size of the structure decreased with an increasing number of FTC [18] .

3.2 Chemical decellularization

Depending on the initial tissue's size, density, cellularity, thickness, and lipid content, chemical treatment-based decellularization's efficacy varies. To speed up the decellularization processes, chemical agents can be mixed with one another, applied simultaneously, or used in conjunction with other decellularizing techniques. The proteomic and biomechanical characteristics of the produced ECM are significantly influenced by the order in which tissue samples are subjected to various chemical agents in protocols that employ several decellularizing agents. The nonionic detergent Triton X-100 and the ionic detergent Sodium Dodecyl Sulfate (SDS) are the most often used detergents for decellularization [19,20]. SDS breaks protein-protein interactions and disintegrates cell membranes, whereas Triton X-100 eliminates cellular content by impairing lipid-lipid and protein-lipid connections without impacting protein-protein interactions. Any SDS-based approach must consequently optimize SDS concentration and tissue exposure period, as higher exposure is directly related to decreasing ECM biomechanical characteristics. Ionic detergents, such as SDS, have the advantage of being able to successfully remove nuclear materials in less time than conventional chemical treatments. This comes at the expense of more damage to the ECM matrisome, as SDS treatment may result in a modified microstructure that reduces the biomechanical integrity of the ECM [17]. Normally, decellularization treatments do not use Triton X-100 concentrations more than 1%, while some techniques have demonstrated effectiveness with concentrations that are as high as 3% as long as exposure time is adjusted proportionately. Despite its inability to break down collagens, SDC can successfully decellularize tissues at concentrations of up to 4%. However, larger concentrations of SDC don't lead to higher nuclear elimination rates and result in significant structural integrity damage. Furthermore, SDC decellularizations must be followed by agents such as Deoxyribonuclease (DNase) to minimize DNA agglutination at the tissue surface [14]. The Hudson method is a decellularization technique for peripheral nerves that relies on the use of the detergent Triton X-200 to remove cellular components while preserving the extracellular matrix [21]. McCrary et al. aimed to optimize a new chemical decellularization method for peripheral nerves using sodium deoxycholate (SDC) and other reagents to match the effectiveness of the Hudson method. The optimized process, involving 3% SDC and a 3-hour DNase incubation, successfully preserved extracellular matrix components and removed cellular debris more effectively than the Hudson method. Results showed that the novel method maintained a similar proteomic profile to the Hudson method, reduced cellular protein counts, and did not leave cytotoxic residues, making it a viable alternative for peripheral nerve repair [22].

3.3 Biological decellularization

Some studies have shown that use of detergents like SDS or Triton-X in decellularization process disturbs the collagen and glycosaminoglycan (GAG) in ECM, which significantly decreases its mechanical strength and viscoelasticity [20]. To preserve native content of dECM, enzymes and chelating agents can be used. Shanto et. al used a combination of trypsin and EDTA in decellularization process in cartilage tissue. Distilled water was used to rinse the lyophilized bone fragments and then decellularized in 0.05 % trypsin and 0.02 % EDTA solution with continuous stirring at 37 °C for 24 hours. The process continued with subsequent steps in order to remove the cellular materials. The remaining GAGs and collagen components were analysed using kits the Blycan™ sulphated glycosaminoglycans assay kit, and collagen assay kit. The analysis showed gradual increase in collagen and GAG contents after 3 weeks of in vitro culture with rat bone marrow-derived mesenchymal stem cells (rBMSCs) [23]. DNase, RNase, and benzenes are all frequently used as subsequent processing steps in chemical, physical, or biological decellularization. According to research, the addition of DNase treatment steps can improve the retention of biomechanical characteristics and GAGs in a variety of chemical, enzymatic, and physically based decellularization methods [1].

4 Discussion

Decellularization techniques have made significant strides, enabled the removal of cellular components while preserved the ECM's structural and biochemical integrity. This preservation is crucial for maintaining the bioactivity and mechanical properties of the scaffolds, which are essential for successful tissue engineering applications [24,25]. The integration of decellularized ECM in 3D printing holds the promise of creating scaffolds that closely mimic the native tissue environment, thereby enhancing cell adhesion, proliferation, and differentiation. This bioactivity is vital for the formation of functional tissues and their integration with host tissues post-implantation

[26]. Various decellularization methods, including chemical, enzymatic, and physical approaches, have been explored, each offering distinct advantages and limitations. Physical decellularization methods, while effective at removing cellular material, often compromise the structural integrity of the ECM, making them less ideal for applications requiring high fidelity in matrix architecture. Chemical methods, although efficient at thorough cell removal, can leave behind toxic residues that may interfere with cell viability and function post-bioprinting. Biological decellularization, with its enzymatic specificity, provides a more controlled approach, preserving the biochemical composition and structural properties of the ECM, but may require optimization to ensure complete decellularization [20,21,24]. Ultimately, the choice of decellularization method must strike a balance between the efficiency of cellular removal and the preservation of the ECM's natural properties. This balance is crucial to producing a dECM scaffold that supports cell adhesion, proliferation, and differentiation. Continued research and refinement of these techniques will be essential to advancing the field of bioprinting and enhancing the functionality of engineered tissues [25,26].

5 Conclusion

In conclusion, the advancements in decellularization techniques have significantly impacted the field of tissue engineering, particularly in the context of 3D bioprinting. These techniques have successfully enabled the extraction of cellular components from extracellular matrix (ECM) while retaining its essential structural and biochemical characteristics [22,24,25], which are vital for developing effective tissue scaffolds. The discussion calls for further research to optimize decellularization processes, explore the combination of ECM with other biomaterials to enhance scaffold properties, and conduct comprehensive in vivo studies to validate the clinical efficacy of these bioprinted tissues. The selection of an appropriate decellularization technique is pivotal in the creation of decellularized extracellular matrix for bioprinting applications. Physical, chemical, and biological decellularization methods each offer distinct advantages and drawbacks that must be carefully considered depending on the specific requirements of the tissue engineering application.

Acknowledgement

The state grant agency supported this article - KEGA 018TUKE-4/2023, VEGA 1/0599/22 and APVV – 22-0340.

References

[1] ZHANG, X., CHEN, X., HONG, H., HU, R., LIU, J., LIU, C.: Decellularized extracellular matrix scaffolds: Recent trends and emerging strategies in tissue engineering, *Bioactive Materials*, Vol. 10, pp. 15-31, 2022. https://doi.org/10.1016/j.bioactmat.2021.09.014

[2] THEOCHARIS, A.D., SKANDALIS, S.S., GIALELI, C., KARAMANOS, N.K.: Extracellular matrix structure, *Advanced Drug Delivery Reviews*, Vol. 97, pp. 4-27, 2016. https://doi.org/10.1016/j.addr.2015.11.001

[3] YUE, B.: Biology of the Extracellular Matrix: An Overview, *Journal of Glaucoma*, Vol. 2014, No. 20-23, pp. 1-8, 2014. https://doi.org/ 10.1097/IJG.0000000000000108

[4] MORGAN, M.R., HUMPHRIES, M.J., BASS, M.D.: Synergistic control of cell adhesion by integrins and syndecans, *Nature Reviews Molecular Cell Biology*, Vol. 8, No. 12, pp. 957-969, 2007.

[5] ALCORTA-SEVILLANO, N., MACÍAS, I., INFANTE, A., RODRÍGUEZ, C.I.: Deciphering the Relevance of Bone ECM Signaling, *Cells*, Vol. 9, No. 12, pp. 1-28, 2020. https://doi.org/10.3390/cells9122630

[6] ROSSO, F., GIORDANO, A., BARBARISI, M., BARBARISI, A.: From cell–ECM interactions to tissue engineering, *Journal of Cellular Physiology*, Vol. 199, No. 2, pp. 174-180, 2004.

[7] VALDOZ, J.C., JOHNSON, B.C., JACOBS, D.J., FRANKS, N.A., DODSON, E.L., SANDERS, C., CRIBBS, C.G., VAN RY, P.M.: The ECM: To Scaffold, or Not to Scaffold, That Is the Question, *International Journal of Molecular Sciences*, Vol. 22, No. 23, pp. 1-23, 2021. https://doi.org/10.3390/ijms222312690

[8] LIAO, J., XU, B., ZHANG, R., FAN, Y., XIE, H., LI, X.: Applications of decellularized materials in tissue engineering: advantages, drawbacks and current improvements, and future perspectives, *Journal of Materials Chemistry B*, Vol. 8, No. 44, pp. 10023-10049, 2020. https://doi.org/10.1039/D0TB01534B

[9] MOFFAT, D., YE, K., JIN, S.: Decellularization for the retention of tissue niches, *Journal of Tissue Engineering*, Vol. 13, No. 1, pp. 1-11, 2022. https://doi.org/10.1177/20417314221101151

[10] ZIMMERMANN, D.R., DOURS-ZIMMERMANN, M.T.: Extracellular matrix of the central nervous system: from neglect to challenge, *Histochemistry and Cell Biology*, Vol. 130, No. 4, pp. 635-653, 2008. https://doi.org/10.1007/s00418-008-0485-9

[11] KLAK, M., KOSOWSKA, K., BRYNIARSKI, T., ŁOJSZCZYK, I., DOBRZAŃSKI, T., TYMICKI, G., FILIP, A., SZCZEPANKIEWICZ, A.A., OLKOWSKI, R., KOSOWSKA, A., BERMAN, A., KAMIŃSKI, A., WSZOŁA, M.: Bioink based on the dECM for 3D bioprinting of bionic tissue, the first results obtained on murine model, *Bioprinting*, Vol. 28, No. 1, p. e00233, 2022. https://doi.org/10.1016/j.bprint.2022.e00233

[12] HOSHIBA, T., CHEN, G., ENDO, C., MARUYAMA, H., WAKUI, M., NEMOTO, E.,

KAWAZOE, N., TANAKA, M.: Decellularized extracellular matrix as an in vitro model to study the comprehensive roles of the ECM in stem cell differentiation, *Stem Cells International*, Vol. 2016, No. 1, pp. 1-11, 2016. https://doi.org/10.1155/2016/6397820

[13] JIANG, S., ZHUANG, Y., CAI, M., WANG, X., LIN, K.: Decellularized extracellular matrix: A promising strategy for skin repair and regeneration, *Engineered Regeneration*, Vol. 4, No. 4, pp. 357-374, 2023. https://doi.org/10.1016/j.engreg.2023.05.001

[14] KIM, M.K., JEONG, W., LEE, S.M., KIM, J.B., JIN, S., KANG, H.-W.: Decellularized extracellular matrix-based bio-ink with enhanced 3D printability and mechanical properties, *Biofabrication*, Vol. 12, No. 2, p. 025003, 2020. https://doi.org/10.1088/1758-5090/ab5d80

[15] AL-HAKIM KHALAK, F., GARCÍA-VILLÉN, F., RUIZ-ALONSO, S., PEDRAZ, J.L., SAENZ-DEL-BURGO, L.: Decellularized Extracellular Matrix-Based Bioinks for Tendon Regeneration in Three-Dimensional Bioprinting, *International Journal of Molecular Sciences*, Vol. 23, No. 21, pp. 1-23, 2022. https://doi.org/10.3390/ijms232112930

[16] ERGUN, C., PARMAKSIZ, M., VURAT, M.T., ELÇIN, A.E., ELÇIN, Y.M.: Decellularized liver ECM-based 3D scaffolds: Compositional, physical, chemical, rheological, thermal, mechanical, and in vitro biological evaluations, *International Journal of Biological Macromolecules*, Vol. 200, pp. 110-123, 2022. https://doi.org/10.1016/j.ijbiomac.2021.12.086

[17] HOSHIBA, T.: Cultured cell-derived decellularized extracellular matrix (cultured cell-derived dECM): Future applications and problems—a mini review, *Current Opinion in Biomedical Engineering*, Vol. 17, p. 100256, 2021. https://doi.org/10.1016/j.cobme.2020.100256

[18] LUO, P., HUANG, R., WU, Y., LIU, X., SHAN, Z., GONG, L., DENG, S., LIU, H., FANG, J., WU, S., WU, X., LIU, Q., CHEN, Z., YEUNG, K.W.K., QIAO, W., CHEN, S., CHEN, Z.: Tailoring the multiscale mechanics of tunable decellularized extracellular matrix (dECM) for wound healing through immunomodulation, *Bioactive Materials*, Vol. 28, pp. 95-111, 2023. https://doi.org/10.1016/j.bioactmat.2023.05.011

[19] TAYLOR, D.A., SAMPAIO, L.C., FERDOUS, Z., GOBIN, A.S., TAITE, L.J.: Decellularized matrices in regenerative medicine, *Acta Biomaterialia*, Vol. 74, pp. 74-89, 2018. https://doi.org/10.1016/j.actbio.2018.04.008

[20] KIM, B.S., KIM, H., GAO, G., JANG, J., CHO, D.-W.: Decellularized extracellular matrix: a step towards the next generation source for bioink manufacturing, *Biofabrication*, Vol. 9, No. 3, p. 034104, 2017. https://doi.org/10.1088/1758-5090/aa7e93

[21] KIM, J.K., KOH, Y.-D., KIM, J.O., SEO, D.H.: Development of a decellularization method to produce nerve allografts using less invasive detergents and hyper/hypotonic solutions, *Journal of Plastic, Reconstructive & Aesthetic Surgery*, Vol. 69, No. 12, pp. 1690-1696, 2016. https://doi.org/10.1016/j.bjps.2016.08.010

[22] MCCRARY, M.W., VAUGHN, N.E., HLAVAC, N., SONG, Y.H., WACHS, R.A., SCHMIDT, C.E.: Novel sodium deoxycholate-based chemical decellularization method for peripheral nerve, *Tissue Engineering Part C: Methods*, Vol. 26, No. 1, pp. 23-36, 2020. https://doi.org/10.1089/ten.tec.2019.0188

[23] SHANTO, P.C., PARK, S., PARK, M., LEE, B.-T.: Physico-biological evaluation of 3D printed dECM/TOCN/alginate hydrogel based scaffolds for cartilage tissue regeneration, *Biomaterials Advances*, Vol. 145, p. 213239, 2023. https://doi.org/10.1016/j.bioadv.2022.213239

[24] KEANE, T.J., SWINEHART, I.T., BADYLAK, S.F.: Methods of tissue decellularization used for preparation of biologic scaffolds and in vivo relevance, *Methods*, Vol. 84, pp. 25-34, 2015. https://doi.org/10.1016/j.ymeth.2015.03.005

[25] MENDIBIL, U., RUIZ-HERNANDEZ, R., RETEGI-CARRION, S., GARCIA-URQUIA, N., OLALDE-GRAELLS, B., ABARRATEGI, A.: Tissue-specific decellularization methods: rationale and strategies to achieve regenerative compounds, *International Journal of Molecular Sciences*, Vol. 21, No. 15, p. 5447, 2020. https://doi.org/10.3390/ijms21155447

[26] BAIGUERA, S., DEL GAUDIO, C., DI NARDO, P., MANZARI, V., CAROTENUTO, F., TEODORI, L.: 3D printing decellularized extracellular matrix to design biomimetic scaffolds for skeletal muscle tissue engineering, *BioMed Research International*, Vol. 2020, No. 1, p. 2689701, pp. 1-13, 2020. https://doi.org/10.1155/2020/2689701

Review process
Single-blind peer review process.

https://doi.org/10.22306/atec.v10i3.208 *Received: 21 June 2024; Revised: 26 Aug. 2024; Accepted: 15 Sep. 2024*

Production of biomedical filament and mechanical testing of samples produced by FFF additive technology

Tomas Balint
Biomedical Engineering and Measurement Department, Faculty of Mechanical Engineering, Technical University of Košice, Letná 1/9, 042 00, Košice, Slovak Republic, EU, tomas.balint@tuke.sk (corresponding author)
Jozef Zivcak
Biomedical Engineering and Measurement Department, Faculty of Mechanical Engineering, Technical University of Košice, Letná 1/9, 042 00, Košice, Slovak Republic, EU, jozef.zivcak@tuke.sk
Miroslav Kohan
Biomedical Engineering and Measurement Department, Faculty of Mechanical Engineering, Technical University of Košice, Letná 1/9, 042 00, Košice, Slovak Republic, EU, miroslav.kohan@tuke.sk

Keywords: PLA, polymer, filament, filament maker, extrusion.
Abstract: This scientific study, which brings completely new results, is characteristically divided into chapters where the authors deal with the extrusion mechanism, filament production, 3D printing of samples, and mechanical testing of samples. This research deals with a current topic in the field of production and testing of filaments composed of biodegradable polymers based on custom made PLA/PHB material. The authors of this study managed to produce and test a new type of biomaterial in the form of a filament called PLA BIOPOLYMER 20. The individual components forming this new type of material are described in the detailed statistics of this scientific article. After optimizing the parameters during single-screw extrusion on a filament maker, where the extrusion temperatures were set to 180° and the subsequent additive manufacturing of samples using FFF technology was started, where "dogbone type 5A" samples were printed. The authors managed to optimize the parameters of additive manufacturing and achieve significant results, which are also represented by individual printed samples, intended for subsequent mechanical testing, specifically for tensile testing. Important testing of materials for mechanical tensile tests was carried out according to generally applicable standards STN EN ISO 527-2, on the Inspekt table 5kN device. By mechanical testing, the individual stresses of the samples were determined. The average stress was 5.28 MPa. The authors compared the values obtained with samples printed from the new type of PLA BIOPOLYMER 20 material with the tension obtained with samples printed from pure PLA filament without admixture of other components. These tests are intended to determine the future application of the given material. This article brings new knowledge in the given field.

1 Introduction

The extrusion process can also be defined as a production technology in which metal or plastic materials are pushed through a fixed cross-sectional profile to create a continuous strip of shaped product (filament). The extrusion process begins with the introduction of material in the form of granules, pellets or powders from hoppers into the extruder zone. The melting process then begins through the heat generated by the mechanical energy generated by the rotating screws and heaters located along the head. The molten ones are then pressed into a matrix, which structures the materials into a hard pipe material during the cooling process. A single-screw extruder is the most common type of extruder and offers relatively low investment costs for companies involved in extruding materials intended for biodegradable purposes. If higher production and higher performance are required, twin-screw extruders are used. The easiest way to increase the throughput of the extruder is to increase the speed of the screw. This easy solution usually results in poor melt quality caused by exceeding the melting capacity of the screw design and degradation caused by high melt temperature. Using a screw with a smaller diameter can offer several advantages for achieving higher throughput at a higher screw speed. One of the important advantages of a smaller diameter extruder is better heat transfer characteristics. Higher output at higher screw speed can be achieved by using a smaller diameter extruder. This offers better heat transfer characteristics [1-6]. A well-designed, developed screw design improves product quality and reduces the time needed to design and optimize the extrusion process, resulting in lower costs. Figure 1 shows a type of single-screw extruder. In twin-screw extruders, clogging of the material can be prevented, but in single-screw extruders, the material is retained much longer than in twin-screw extruders. A twin-screw extruder has about three times the material output. Theoretically, the material flow process can be divided into four sections: (a) extruder filling, (b) mass transport, (c) flow through the die, and (d) exit from the die and subsequent processing. The material processing time in the extruder is called the material distribution time. The residence time distribution is an important parameter for product quality. Most commercial extruders provide a choice of screws or interchangeable sections that change the configuration of the feed, transition and metering zones.

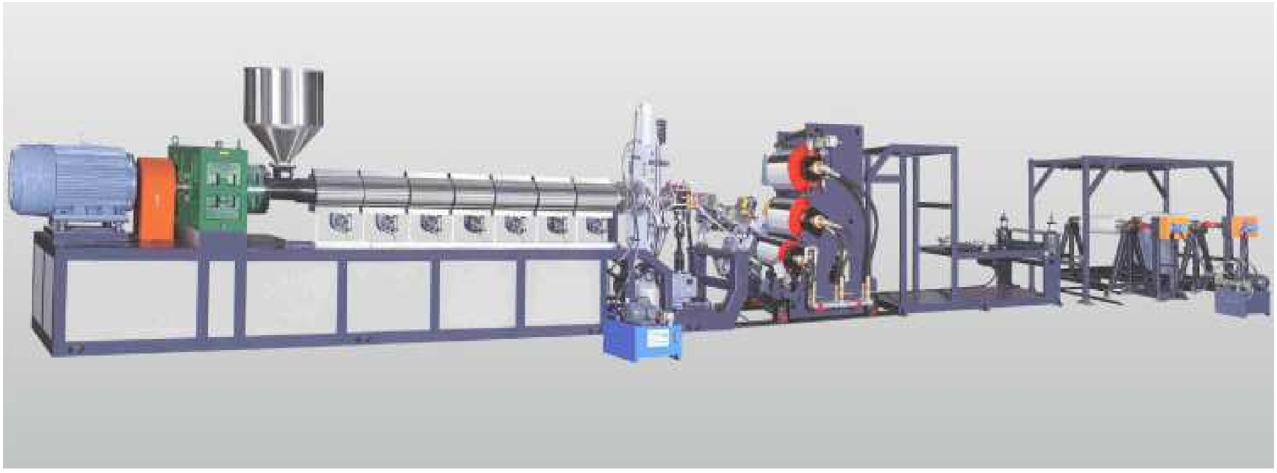

Figure 1 Single-thread industrial system for the production of filaments [1]

1.1 Characteristics of materials

Our filament consists of PLA/PHB polymers and added plasticizer with thermoplastic starch. The distribution and weight ratio of all materials is one to 25 percent. PLA material is easy to use and will ensure a relatively high-quality 3D model. It is biodegradable in nature and is made from corn starch. The thermal properties of PLA play a significant role in its performance during the 3D printing process. One of the key thermal properties of PLA is its glass transition temperature, which is the temperature at which the material changes from a hard, glassy state to a soft, rubbery state. For PLA it is usually around 60°C. Another important thermal property of PLA is its melting point. It is the temperature at which the material changes from a solid state to a liquid state. For PLA, the melting temperature is typically in the range of 130–180 °C. This relatively low melting point is one of the reasons why PLA is preferred in 3D printing. It allows easier extrusion through the printer nozzle and better control over the printing process. PLA is a thermoplastic polymer characterized by high mechanical resistance, suitable biocompatibility and bioresorbability. It is produced from renewable and non-toxic sources of raw materials. Lactic acid (LA) is converted to PLA by condensation polymerization. Due to the chiral nature of LA and the two asymmetric centers it has, it can form in a wide variety of forms and also has the following isomers: L, D and D, L isomers as well as the D isomer. Compared with other aliphatic polyesters, PLA has demonstrated many superior properties, such as high mechanical strength and modulus, biodegradability, biocompatibility, and easy processing. In Figure 2 we can see the pla structure [7-9].

PHB materials are mechanically stiff and brittle, with low thermal stability and a high degree of crystallinity. Many PHB plastics have properties that are similar to petroleum polymers - polypropylene (PP) and polyethylene (PE) [10]. Feedstocks for the production of PHB biopolymers include renewable and sustainable sources such as food waste. When exposed to designated active biological environments, these factors, combined with its biocompatibility and predisposition to biodegradation, make PHB a leading candidate as an alternative to synthetic polymers. Figure 3 shows us the structure of the PHB [11-14].

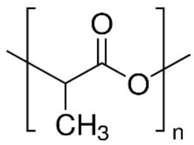

Figure 2 PLA structure [11]

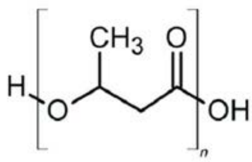

Figure 3 PHB structure [11]

2 Methodology of extrusion and 3D printing

2.1 Filament extrusion

Filament production is a multi-step process. We performed filament extrusion on a single-screw extruder from 3Devo. As an input material, we had medically certified pellets, which were composed, as mentioned above, from PLA/PHB materials with the addition of a plasticizer. The extrusion temperature was set to 180°C on all four extrusion bodies of the extruder. We set the screw rotation speed to 3.0 RPM. In Figure 4 we see the material flow. Figure 5 shows us the finally manufactured filament BIOPOLYMER 20.

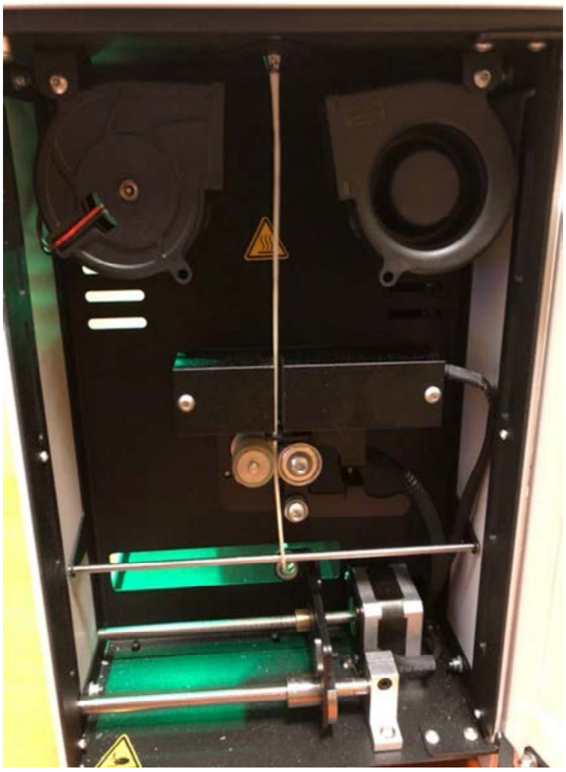

Figure 4 Material flow

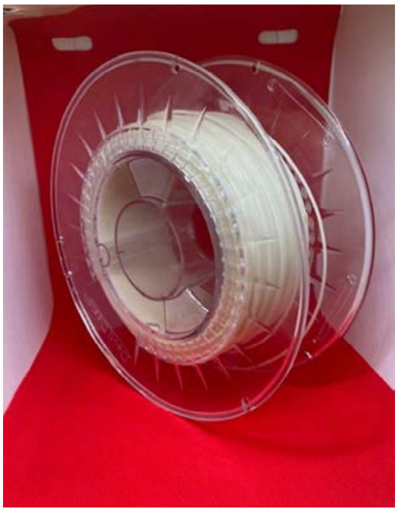

Figure 5 Final filament BIOPOLYMER 20

2.2 3D printing of samples

Samples for mechanical testing were produced using additive FFF technology on a Trilab printer. These were dogbone 5A samples. We set the printing temperature to 175°C and the substrate temperature to 60°C. We set the print speed to 1200mm/s. The modeling of the samples was performed in the Symplify software (Figure 6). In total, more than 20 samples were printed (Figure 7).

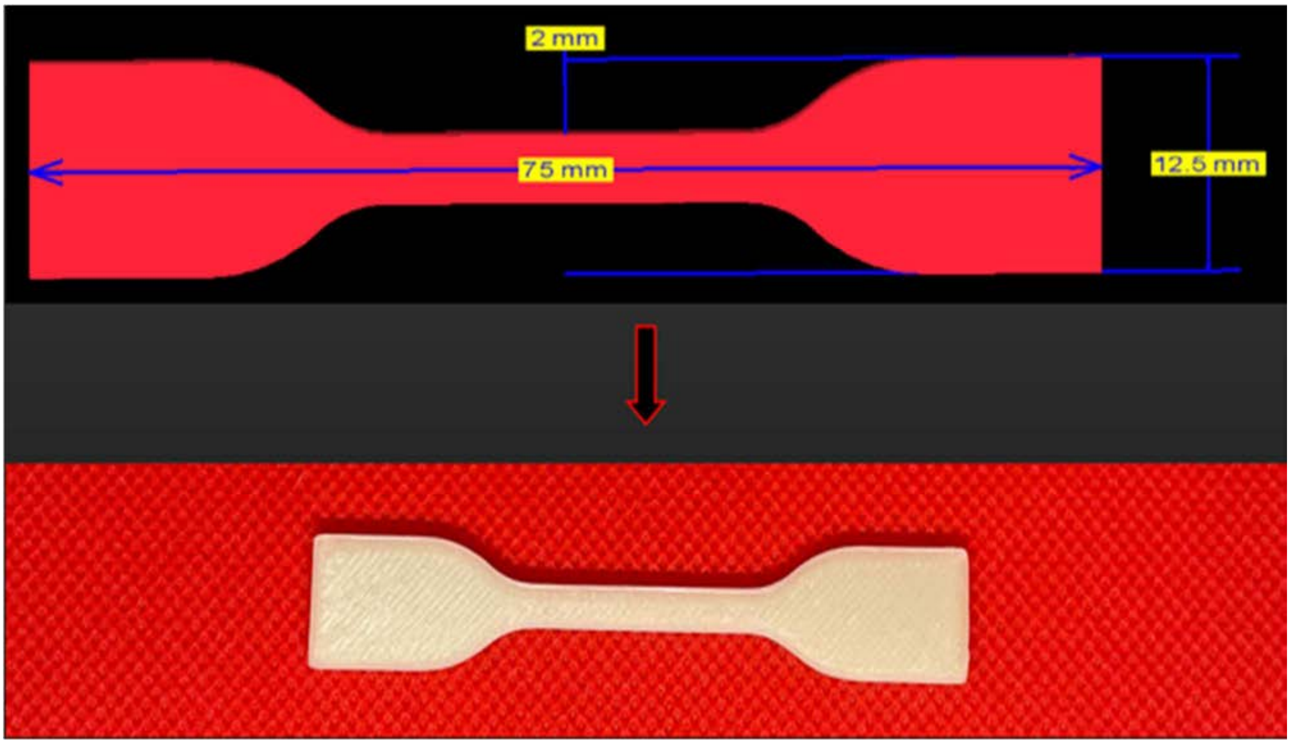

Figure 6 Type 5A dogbone sample model

Figure 7 Final printed samples using FFF technology

3 Mechanical testing characterisation

Important testing of materials for mechanical tensile tests was carried out according to generally applicable standards STN EN ISO 527-2, on the Inspekt table 5kN device. The load speed was set to 2 mm per minute. About 20 samples were mechanically tested, where Table 1 gives us the results of tension values with average of 5.28 MPa.

Table 1 Technical specifications

Tested sample	***PLA/PHB [MPa] Tension***
1	4.57
2	5.45
3	5.11
4	5.23
5	5.46
6	5.53
7	5.11
8	5.12
9	5.09
10	5.02
11	4.90
12	5.26
13	5.39
14	5.61
15	5.18
16	5.45
17	5.25
18	5.66
19	5.66
20	4.99
21	5.22
22	5.18
Average	**5.28**

4 Conclusion

The results in this study significantly contribute to the field of material production through extrusion on a filament maker device, 3D printing using FFF technology, and determine the future of use by mechanically determining the strength of the material. Printing biodegradable materials provides precision and flexibility in creating complex structures. Material based on PLA and PHB is biodegradable to some extent. This is what motivated us to implement and solve the problem of this topic.

The facts we have obtained can be of great benefit to the practice in the future. The biodegradable material created has the potential to influence the medical industry in the future. For example, for access to more personalized treatment procedures, or also the possible use of material in the human body for the regeneration of bone tissue. These findings open the door for further possible research into the evaluation of mechanical, biological and biocompatible properties.

Acknowledgement
This scientific study was created thanks to support under the Operational Program Integrated In-frastructure for the project "Center for Medical Bioadditive Research and Production (CEMBAM), code ITMS2014 +: 313011V358, co-financed by the European Regional Development Fund", with the support of the project Op-erational Program Integrated Infrastructure for the project: Open Scientific Community for Mod-ern Interdisciplinary Research in Medicine (OPENMED), code ITMS2014 +: 313011V455, co-financed by the European Regional Development Fund and thanks to support under the Opera-tional Program Integrated infrastructure for the project: Center for Advanced Therapies of Chronic Inflammatory Diseases of the Musculoskeletal System (CPT ZOPA), code ITMS2014 +: 313011W410, co-financed by the European Regional Development Fund and APVV SK-CZ-RD-21-0056 Bioresorbable materials for additive manufacturing of vessel substituents and their biomechanical characterization and thank to project VEGA 1/0599/22 - Design and biomechanical analysis of personalized instruments for arthroscopic applications.

References

[1] SURISAENGA, J., KANABENJAA, W., PASSORNRAPRASITA, N., AUMNATEB, C. POTIYARAJ, P.: Polyhydroxybutyrate/polylactic acid blends: An alternative feedstock for 3D printed bone scaffold model, *Journal of Physics: Conference Series*, Vol. 2175, pp. 1-6, 2022. https://doi.org/10.1088/1742-6596/2175/1/012021

[2] SHAMAZ, M., SHAMAZ, B.H.: Bone tissue engineering and bony scaffold, *International Journal of Dentistry and Oral Health*, Vol. 2015, No. 1, pp. 15-20, 2015.

https://doi.org/10.25141/2471-657X-2015-1.0001

[3] HUANG, Y.Z., XIE, H.Q., LI, X.: *Scaffolds in Bone Tissue Engineering: Research Progress and Current Applications*, In: Encyclopedia of bone biology, pp. 205-214, 2020.

[4] GUDURIC, V., FÉNELON, M., FRICAIN, J.-CH., CATROS, S.: *Membrane scaffolds for 3D cell culture*, In: Current Trends and Future Developments on (Bio-) Membranes, Elsevier, pp. 157-189, 2020. https://doi.org/10.1016/B978-0-12-814225-7.00007-3

[5] AUSEJO, J.G., RYDZ, J., MUSIOŁ, M., SIKORSKA, W., SOBOTA, M., WŁODARCZYK, J., ADAMUS, G., JANECZEK, H., KWIECIEŃ, I., HERCOG, A., JOHNSTON, B., KHAN, H.R., KANNAPPAN, V., JONES, K.R., MORRIS, M.R., JIANG, G., RADECKA, I., KOWALCZUK, M.: A comparative study of three-dimensional printing directions: The degradation and toxicological profile of a PLA/PHA blend, *Polymer degradation and stability*, Vol. 152, No. June, pp. 191-207, 2018. https://doi.org/10.1016/j.polymdegradstab.2018.04.024

[6] CADDEO, S., BOFFITO, M., SARTORI, S.: Tissue Engineering Approaches in the Design of Healthy and Pathological In Vitro Tissue Models, *Frontiers in Bioengineering and Biotechnology*, Vol. 5, pp. 1-22, 2017. https://doi.org/10.3389/fbioe.2017.00040

[7] HAN, F., WANG. J., DING, L., HU, Y., LI, W., YUAN, Z., GUO, Q., ZHU, C., YU, L., WANG, H., ZHAO, Z., JIA, L., LI, J., YU, Y., ZHANG, W., CHU, G., CHEN, S., LI, B.: Tissue Engineering and Regenerative Medicine: Achievements, Future, and Sustainability in Asia, *Frontiers in Bioengineering and Biotechnology*, Vol. 8, pp. 1-35, 2020. https://doi.org/10.3389/fbioe.2020.00083

[8] ABDULGHANI, S., MITCHELL, G.R.: Biomaterials for In Situ Tissue Regeneration: A Review, *Biomolecules*, Vol. 9, No. 11, pp. 1-24, 2019. https://doi.org/10.3390/biom9110750

[9] MAO, A.S., MOONEY, D.J.: Regenerative medicine: Current therapies and future directions, *Applied Biological Sciences*, Vol. 112, No. 47, pp. 14452-14459, 2015. https://doi.org/10.1073/pnas.1508520112

[10] MATAI, I., KAUR, G., SEYEDSALEHI, A., MCCLINTON, A., LAURENCIN, C.T.: Progress in 3D bioprinting technology for tissue/organ regenerative engineering, *Biomaterials*, Vol. 226, No. January, p. 119536, 2020. https://doi.org/10.1016/j.biomaterials.2019.119536

[11] CUI, X., BOLAND, T., D'LIMA, D.D., LOTZ, M.K.: Thermal inkjet printing in tissue engineering and regenerative medicine, *Recent Pat Drug Deliv Formul*, Vol. 6, No. 2, pp. 149-155, 2012. https://doi.org/10.2174/187221112800672949

[12] TAMEZANI, H., MIRJAMALI, S.M., HE, Y.: Simulations of Extrusion 3D Printing of Chitosan Hydrogels, *Applied Sciences*, Vol. 12, No. 15, pp. 1-15, 2022. https://doi.org/10.3390/app12157530

[13] ZAY, Y.W.D., LI, M.Y., TAN, M.J.: Effect of printing parameters in 3D concrete printing: Printing region and support structures, *Journal of Materials Processing Technology*, Vol. 271, pp. 261-270, 2019. https://doi.org/10.1016/j.jmatprotec.2019.04.007

[14] CLAIRE, S.: ICON Reveal Design for Quirky 3D Printed Texas Campground Hotel on 62 Acre Site, 3Dnatives, *3D Printing News Architecture*, Vol. 2023, No. March, 2023.

Review process

Single-blind peer review process.

Acta Tecnología - International Scientific Journal about Technologies
Volume: 10 2024 Issue: 3 Pages: 93-98 ISSN 2453-675X

https://doi.org/10.22306/atec.v10i3.212 *Received: 01 July 2024; Revised: 02 Sep. 2024; Accepted: 18 Sep. 2024*

Investigation of the influence of mechanical milling on magnetic properties of Fe powders

Livia Provazkova
Institute of Manufacturing Management, Faculty of Manufacturing Technologies with the seat in Prešov, Technical University of Košice, Bayerova 1, 080 01, Prešov, Slovak Republic, EU,
livia.provazkova@tuke.sk (corresponding author)
Marian Reiffers
Department of Physics, Mathematics and Technologies, Faculty of Humanities and Natural Sciences, University of Prešov, 17. novembra 15, 080 01 Prešov, Slovak Republic, EU, marian.reiffers@unipo.sk
Tetiana Rudeichuk
Institute of Manufacturing Management, Faculty of Manufacturing Technologies with the seat in Prešov, Technical University of Košice, Bayerova 1, 080 01, Prešov, Slovak Republic, EU,
tetiana.rudeichuk@tuke.sk
Denisa Oleksakova
Institute of Manufacturing Management, Faculty of Manufacturing Technologies with the seat in Prešov, Technical University of Košice, Bayerova 1, 080 01, Prešov, Slovak Republic, EU,
denisa.oleksakova@tuke.sk

Keywords: soft magnetic materials, hysteresis loop, magnetic properties, iron powder.

Abstract: Nowadays, there is a global search for electromagnetic gadgets that are affordable, eco-friendly, and energy-efficient. This motivates engineers and scientists to develop new materials or enhance those that already exist. Fe-based soft magnetic materials are a significant class of soft magnetic materials that are essential to many energy-related industrial applications, including motors, converters, and electric transformers. This article focuses on the general characterization of magnetic materials, their magnetic properties and the analysis of the influence of mechanical milling of Fe powders prepared by mechanical milling in two different sizes (sample 1 – smaller then < 400 μm and sample 2 greater than > 400 μm). The experimentally obtained hysterical curves of ground Fe powders are measured using the Vibratimg Sample Magnetometer (VSM).

1 Introduction

Nowadays, we observe worldwide search for electromagnetic devices that are energy efficient, environmentally friendly and economically viable. This forces scientists and engineers to improve existing materials or discover entirely new materials [1].

A new generation of energy materials is needed in order to pursue higher efficiency in energy transformation and conversion [2]. Soft magnetic materials are an essential component of human civilization and have been used in many important technical applications, including the production and conversion of electricity [3].

Soft magnetic materials can change their magnetic polarization quickly in response to mild magnetic fields. They are mostly utilized to increase or channel the flux created by an electric current and usually have low inherent coercivity [2-4].

Transformers, converters, inductors, motors, generators, and even sensors are just a few of many electromagnetic distribution, conversion, and generating devices that employ these magnetic materials [5]. The expedited development and desing of novel energy materials has drawn a lot of interest in the materials science community nowadays because of the numerous societal and environmental issues we are currently facing [2,6].

In this study, we used mechanical milling to produce microcrystalline elemental iron powders. Iron powder with purity of 99.98% and particle size less than 400 μm (sample 1) and particle size greater than 400 μm (sample 2) were prepared and used for the experiment. We used mechanical milling in our study to create microcrystalline elemental iron particles. Specifically, sample 1 (particle size less than 400 μm) and sample 2 (particle size higher than 400 μm) of 99.98% pure iron powder were used in the experiment. The purpose of this work is to present a broad review of magnetic materials with an emphasis on magnetic soft materials, and to compare the magnetic characteristics of the obtained Fe powders using primary magnetization and hysteresis loop based on their size.

2 Magnetic materials

Magnetic materials are divided into diamagnetic, paramagnetic, ferromagnetic, ferrimagnetic and antiferromagnetic on the basis of their internal structure (arrangement of electrons in atoms). Ferromagnetics are among the most widely used materials in the manufacture of various technologies because of their atypical properties such as magnetic hysteresis (hysteresis loop) [7]. The shape of the hysteresis loop indicates the magnetic substance in question. Magnetic hysteresis is the dependence of the induction $\vec{B}$ of the magnetic material from the magnetic field strength $\vec{H}$ and expresses a non-linear relationship between $\vec{B}$ and $\vec{H}$, also that induction $\vec{B}$ lags behind the magnetic field strength $\vec{H}$ [8].

Based on the hysteresis loop, with the help of which we find the dependence of the magnetic induction $\vec{B}$ on the magnetic field strength $\vec{H}$, two categories of these ferromagnetic substances are distinguished, namely soft and hard magnetic ferromagnetics [9-10].

- Soft ferromagnetic materials are usually iron-based and are obtained by pressing a soft magnetic powder with a dielectric (electroinsulating) binder (matrix). These are materials that are easily magnetized and demagnetized, making them useful when it is necessary to switch the magnetic field quickly and easily, for example, in motors [10].
- Hard (permanent) ferromagnetic materials, most commonly Nd-Fe-B, are formed by bonding hard magnetic powder to a dielectric (electrical insulating) binder. These are materials that retain their magnetisation. If these permanent magnetic materials were used in a situation where it is necessary to switch the magnetic field rapidly, they would consume a large amount of electric current [10-11].

2.1 Hysteresis loop

The hysteresis loop expresses the dependence of the magnetic induction $\vec{B}$ on the magnetic field strength $\vec{H}$. The shape of the loop characterizes the type of material. A wide hysteresis loop characterises a magnetically hard material where a high field strength is required for remagnetisation. Conversely, a narrow loop is characteristic of magnetically soft materials (Figure 1) [8-9]. In Figure 1, the magnetic moment *M* is a measure of the material's magnetization. It displays the amount of magnetization that a material exhibits when exposed to a magnetic field. H_k represent coercive force and H_0 frequently denotes the material's exposure to an external magnetic field.

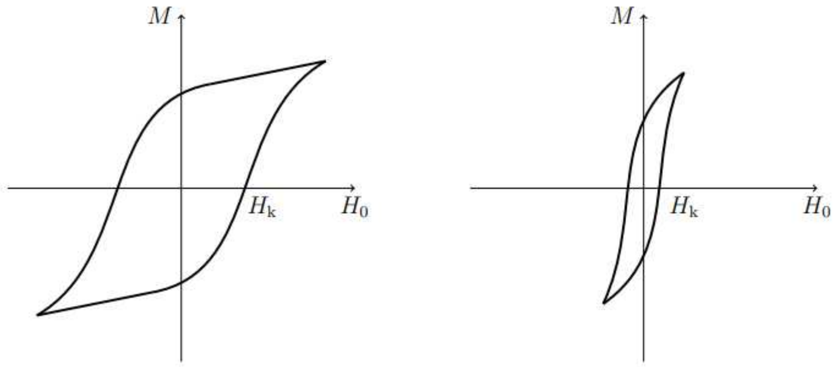

Figure 1 Hysteresis loop of magnetically hard and soft materials [8]

Figure 2 shows the hysteresis loop even with the initial magnetization. The hysteresis loop is labeled by No. 2 and in red, the initial magnetization curve is labeled by No. 1.

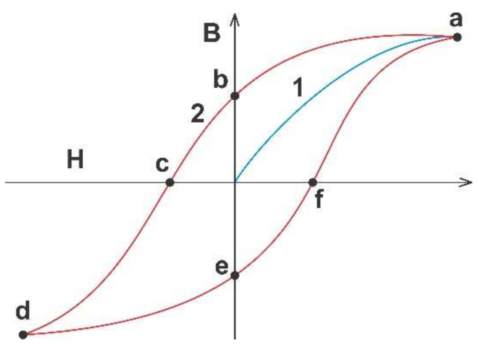

Figure 2 Hysteresis loop

The course of the magnetization curve is described by the letters *a to f*. After the initial magnetization, the *material* is saturated at point *a* . As the magnetic field strength decreases, the magnetic induction $\vec{B}$ also decreases up to point *b*. At this point, there is no magnetic field acting on the material, but the magnetic induction is not zero - that is, the material has remained partially magnetized. Such an induction is called remanent. As the strength of the magnetic field increases to negative values, the curve passes through point c. At this point, a magnetic field is applied to the material, but the magnetic induction in the material is zero - but the material still has some polarisation $\vec{I}$. The magnetic field strength required to remove the magnetic induction (magnetic field of opposite direction) in a material is called the coercivity H_c. Consequently, as the intensity increases to negative values, at point *d* the magnetic domains in the material are magnetized in the opposite direction to point *a*. Further, the magnetic field strength is varied from negative to positive values. Point *e* on the curve corresponds to point *b* and point *f* corresponds to point *c*. The initial magnetization curve (no. 1) is obtained from a completely demagnetized material which is placed in a gradually increasing magnetic field. The change in the magnetic field strength must be in one direction only to avoid the curve being depreciated [9-11].

2.2 Coercivity

Coercivity and remanence are plotted in Figure 2. Coercivity H_c is indicated on the loop by point *c*. This property indicates how much magnetic field strength is required to achieve zero magnetic induction $\vec{B}$ in a material that has already been magnetized. The remanence (remanent magnetization of M_r) B_r is indicated on the curve by point *b*. This property indicates how much magnetic induction remains in the material after the external magnetic field $\vec{H}$ is removed. In the case of the maximum area hysteresis loop, its ends correspond to the saturation state of the ferromagnetic substance. The values of coercivity H_c and remanence B_r are characteristic of magnetically soft and magnetically hard materials, with H_c > 1000 A.m^{-1} for hard materials and H_c < 1000 A.m^{-1} for soft materials [12].

3 Methodology

Ball milling is a widely used technique in the field of materials science and engineering to synthesize various advanced materials [13-15]. The process involves mechanical activation of powders through repeated collision of grinding balls with powder particles, thereby reducing the particle size and creating new interfaces. While the ball milling process is relatively simple, there are several critical processing parameters that can significantly affect the quality and properties of the final product [16]. These parameters include mill type, milling time and speed, type and viscosity of milling medium, milling temperature, Ball to Powder Ratio (BPR) and atmosphere. In our experiment, we used the PM100 planetary ball mill from Retsch (Figure 3) because it has a powerful speed-controlled grinding action, which allows for a reproducible result [17-18].

Figure 3 Planetary ball mill Retsch PM100 (in Institute of Physics, Faculty of Science, P. J. Šafárik University in Košice)

3.1 Experimental materials

To study and compare the magnetic properties, we prepared two samples (sample 1 and sample 2) of pure iron powders. One sample was prepared from pure iron granules of 1-2mm size and high purity (99.98% purity, Alfa-Aesar Co.), which was then processed by mechanical grinding in a ball mill. For the second sample we used as starting material a reduced Fe powder of high purity (99.9% purity, Centralchem), which, unlike the first sample, was passed through a reamer without processing in a mechanical mill.

We prepared two samples of pure iron powder in order to investigate and compare the magnetic properties. One sample, made of high-purity (99.98% pure, Alfa-Aesar Co.) pure iron granules with a size of 1-2 mm, was mechanically ground in a ball mill. Unlike the first sample, which was processed in a mechanical mill, the second sample was prepared without the need for a mechanical mill by passing through a reamer and using a reduced Fe powder of high purity (99.9% purity, Centralchem) as the starting material.

3.2 Preparation of Fe powders

The first sample that we weighed and prepared was iron granules of 1-2 mm in size, which were then dumped into the lubricator along with the pre-weighed steel balls. The chosen weight ratio of the beads was in the ratio of 9:1 (BPR). High-energy ball milling of iron pellets and steel balls was carried out at room temperature using a planetary ball mill which combines high friction with impact at a speed of 500 rpm. A stainless steel grinder and hardened steel balls were used. The weight of the balls was 178.28 g, the weight of the iron pellets was 19.81 g and the total weight of pellets, balls and grinding mill was 4227.4 g. The grinding process itself lasted 2 hours with 10 second breaks due to material and mill temperature stabilization and with reverse rotation in each cycle for 70 seconds for optimum mixing. One of the disadvantages of ball milling is that long grinding times are often required to achieve the desired particle size and distribution, resulting in extended processing times. In addition, friction and collisions between the balls and the material during grinding can generate a significant amount of heat which can affect the stability and properties of the material being processed, especially for heat-sensitive materials. Therefore, the selection of parameters in the ball milling process is a key factor in determining the final product properties. After the milling process was completed, we re-weighed separately the balls (179.56g) and the resulting iron powder (17.07g). We then transferred this powder into a reamer and allowed it to digest for 3 minutes.

The sample 2 was prepared from atomized iron powder with size below 400 μm whose weighed weight was 10.038g. This powder was poured into a reamer and allowed to strain for 5 minutes. Finally, we sieved the strained iron powder into a glass slide and weighed its weight (9.96g). The addition process is shown in Figure 4.

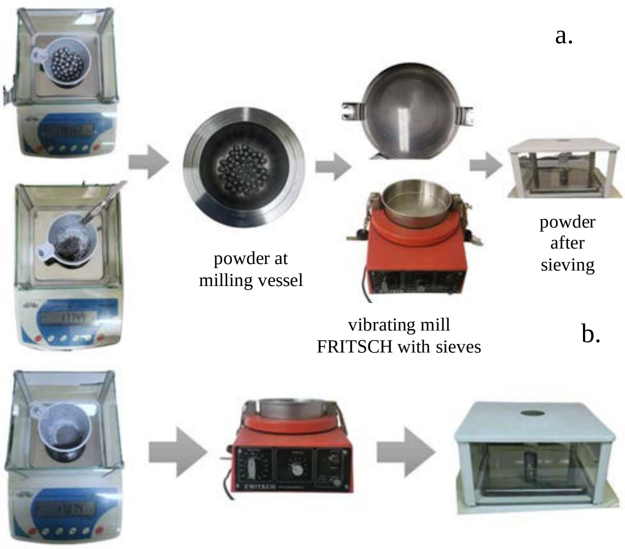

Figure 4 Process for the preparation of a. Fe granules 1-2 mm in size and b. Fe reduced powder

4 Experimental part

Magnetic properties of the sample 1 and the sample 2 were measured using a Vibrating Sample Magnetometer (VSM) on a DYNACOOL device of Quantum design in the temperature range of 200 to 390 K and in the dc applied magnetic field range of -2.39 to 2.39 MA/m. We carried out our measurements in this temperature range to approximate real situations [19].

We exposed two iron powder samples (Fe reduced powder with particles less than 400 μm - sample 1 and non – milled Fe powder with particles more than 400 μm - sample 2) to temperatures of 200 K, 300 K, and 390 K in order to study and compare the magnetic properties (primary magnetization and hysteresis loop).

Figure 5 for the sample 1 and Figure 6 for the sample 2 illustrates the experimentally measured dependence of magnetic moment on magnetic field from -2,39 MA/m to 2,39 MA/m for various temperatures (200 K, 300 K, and 390 K).

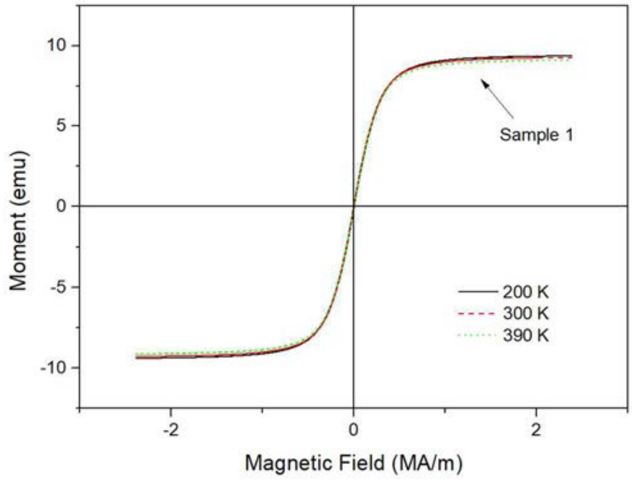

Figure 5 Effect of temperature on the magnetic hysteresis loop of the sample 1

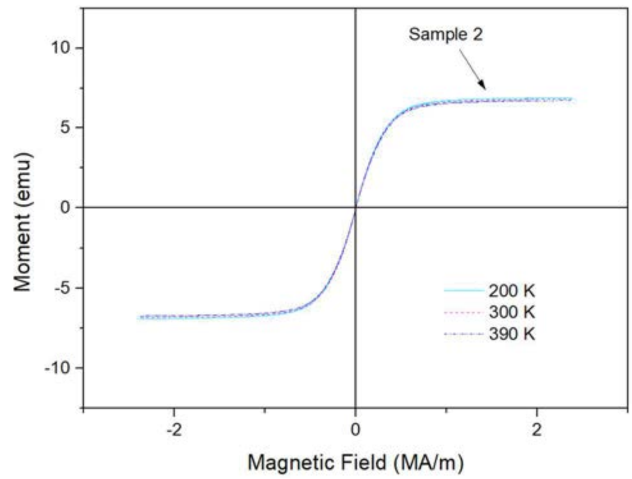

Figure 6 Effect of temperature on the magnetic hysteresis loop of the sample 2

The sample 1 (Figure 5) with a particle size less than 400 μm has larger values of the magnetic moment at the selected temperatures than the sample 2 with a particle size more than 400 μm (Figure 6), which demonstrating the clear effect of temperature on the shape of the magnetization curves. It is reasonable to assume that the mechanical milling process raises the magnetization value. Defects introduced into the sample during the milling process may be the cause. The sample 1 has higher value of coercivity. The magnetic moment decreases as the temperature increases for both samples. A clear tendency towards saturation with an applied magnetic field for sample 1 and sample 2 is around 0.9 MA/m for each temperature [20].

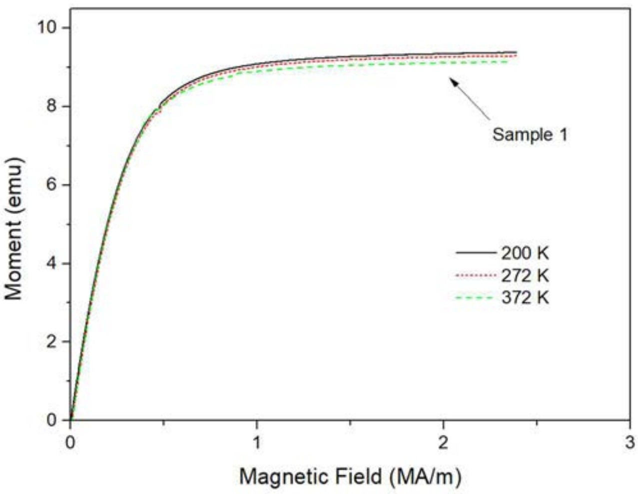

Figure 7 Initial magnetization curve of the sample 1 at different temperatures

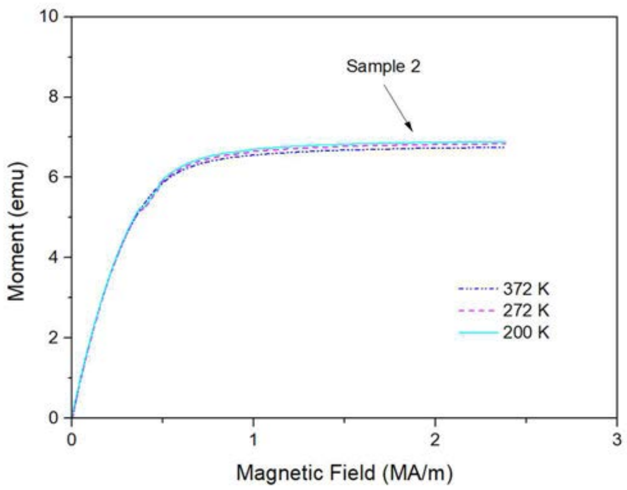

Figure 8 Initial magnetization curve of the sample 2 at different temperatures

The magnetic moment dependency on magnetic field at various temperatures for the sample 1 is shown in Figure 7 and for the sample 2 is shown in Figure 8. The initial magnetization curves (Figure 7 and Figure 8) exhibit a similar pattern to the hysteresis loops (Figure 5 and Figure 6) for both samples 1 and sample 2. It shows that the sample 1, which has smaller particles, exhibits greater magnetization values with rising magnetic field. Consequently, the sample 1 achieves higher magnetization values at lower magnetic field than the sample 2, which has particle sizes larger than 400 µm.

It is reasonable to infer that the mechanical milling process, which produces powdered samples with varying particle sizes, modifies the magnetic properties. Therefore, one method to manufacture a magnetic material with the necessary qualities that is acceptable for further usage (compaction, preparation of magnetic composites, etc.) is through the process of powder metallurgy and mechanical milling.

5 Conclusions

In this work, we investigated how the magnetic properties of iron powders are affected by their particle size. Using a VSM system that measures the magnetic properties of substances, we obtained hysteresis curves and initial magnetization curves for both samples which show how particle size affects the magnetic properties of Fe powders. Particle size variations may not be the only factors affecting magnetic characteristics but also the morphology, purity and possible impurities in the iron powders can all have an impact. We also identified challenges associated with the milling process, such as long processing times and possible thermal effects that may affect the stability and properties of the material.

The results show a connection between magnetic behavior and particle size. In comparison to the sample containing larger particles (more than 400 µm), the sample containing smaller particles (less than 400 µm) showed higher magnetization values and stronger coercivity. This implies that the process of mechanical milling improves the magnetization, because it introduces flaws and produces smaller particles that have a higher surface area and a different domain structure.

We obtained significant knowledge of the magnetic characteristics and behavior of two pure Fe powders of varying sizes under the influence of external magnetic fields at various temperatures by comparing their hysteresis curves and initial magnetization curves. In order to enhance magnetically soft materials, the acquired results can be integrated with the findings from earlier research that examine the compactness of magnetically soft Fe materials with various mechanical milling settings.

Acknowledgement
This work was Funded by the EU NextGenerationEU through the Recovery and Resilience Plan for Slovakia under the project No. 09I03-03-V02-00010, Scientific Grand Agency of Ministry of Education of Slovak Republic and Slovak Academy of Science – project VEGA 1/0403/23 and VEGA 1/0016/24.

References

[1] SUNDAY, K., TAHERI, M.: Soft magnetic composites: recent advancements in the technology, *Metal Powder Report*, Vol. 72, No. 6, pp. 425-429, 2017. https://doi.org/10.1016/j.mprp.2016.08.003
[2] WANG, Y., TIAN, Y., KIRK, T., LARIS, O., ROSS, J. H., NOEBE, R.D., KEYLIN, V., ARRÓYAVE, R.: Accelerated design of Fe-based soft magnetic materials using machine learning and stochastic optimization, *Acta Materialia*, Vol. 194, pp. 144-155, 2020. https://doi.org/10.1016/j.actamat.2020.05.006

[3] LIU, T., LI, F., WANG, A., XIE, L., HE, Q., LUAN, J., HE, A., WANG, X., LIU C.T., YANG, Y.: High performance Fe-based nanocrystalline alloys with excellent thermal stability, *Journal of Alloys and Compounds*, Vol. 776, pp. 606-613, 2019. https://doi.org/10.1016/j.jallcom.2018.10.319
[4] KOCSIS, B., FEKETE, I., VARGA, L.K.: Metallographic and magnetic analysis of direct laser sintered soft magnetic composites, *Journal of Magnetism and Magnetic Materials*, Vol. 501, pp. 1-4, 2020. https://doi.org/10.1016/j.jmmm.2020.166425
[5] ONDERKO, F., BIRČÁKOVÁ, Z., DOBÁK, S.: Magnetic properties of soft magnetic FeSiO2/ferrite composites prepared by wet/dry method, *Journal of Magnetism and Magnetic Materials*, Vol. 543, p. 168640, 2022. https://doi.org/10.1016/j.jmmm.2021.168640
[6] CHOI, M., KIM, M., LEE. K.: The effects of Fe nano-powders on compaction behaviors and magnetic properties of SMCs, *Journal of Magnetism and Magnetic Materials*, Vol. 480, pp. 33-39, 2019. https://doi.org/10.1016/j.jmmm.2019.02.034
[7] CALLISTER, W., RETHWISCH, D.: *Materials Science and Engineering, AN INTRODUCTION*, 10th ed., Hoboken, Wiley, 2018.
[8] HOSFORD, W.F.: *Elementary Materials Science*, Ohio, ASM International, 2013.
[9] KOLENKO, P.: *Úvod do fyziky pevných látek*, Praha, Fakulta jaderná a fyzikálně inženýrská ČVUT, 2023. (Original in Czech)
[10] KIM, Y., ZHAO, X.: Magnetic Soft Materials and Robots, *American Chemical Society*, Vol. 122, No. 5, pp. 5317-5364, 2022. https://doi.org/10.1021/acs.chemrev.1c00481
[11] COEY, J.M.D.: *Magnetism and Magnetic Materials*, Cambridge, Cambridge University Press, 2009.
[12] NGO, T.D.: *Composite and Nanocomposite Materials - From Knowledge to Industrial Applications*, Rijeka, IntechOpen, 2020.
[13] OLEKŠÁKOVÁ, D., KOLLÁR, P., FÜZER, J.: Structure and Magnetic Properties of Powdered and Compacted FeNi Alloys, *Journal of Electrical Engineering*, Vol. 68, No. 2, pp. 327-330, 2017. https://doi.org/10.1515/jee-2017-0024
[14] KUMAR, M., XIONG, X., WAN, Z.: Ball milling as a mechanochemical technology for fabrication of novel biochar nanomaterials, *Bioresource Technology*, Vol. 312, p. 123613, 2020. https://doi.org/10.1016/j.biortech.2020.123613
[15] OLEKŠÁKOVÁ, D., KOLLÁR, P., FÜZER, J., KUSÝ, M., ROTH., S., POLANSKI, K.: The influence of mechanical milling on structure and soft magnetic properties of NiFe and NiFeMo alloys, *Journal of Magnetism and Magnetic Materials*, Vol. 316, No. 2, pp. 838-841, 2007. https://doi.org/10.1016/j.jmmm.2007.03.111
[16] WEI, L.K., ABD RAHIM, S.Z., AL BAKRI ABDULLAH, M.M.: Producing Metal Powder from Machining Chips Using Ball Milling Process, *Materials*, Vol. 16, No. 13, pp. 1-43, 2023. https://doi.org/10.3390/ma16134635
[17] EL-ESKANDARANY, M.S., AL-HAZZA, A., AL-HAJJI, L.A.: Mechanical Milling: A Superior Nanotechnological Tool for Fabrication of Nanocrystalline and Nanocomposite Materials, *Nanomaterials*, Vol. 11, No. 10, p. 2484, pp. 1-35, 2021. https://doi.org/10.3390%2Fnano11102484
[18] MOTOZUKA, S., TAGAYA, M., HAYASHI, K., MORINAGA, M.: Texture formation in iron particles using mechanical milling with graphite as a milling aid, *American Institute of Physics*, Vol. 5, No. 9, pp. 2158-3226, 2015. https://doi.org/10.1063/1.4930915
[19] REIFFERS, M., VILČEK, J, MICHAELI, E., ČURLÍK, I., KLAMÁR, R., ČECH, V., IVANOVÁ, M., KOCO, Š., PASTERNÁK, T., IĽKOVIČ, S., PARMA, L., ŠEBEŇ, V., ŠTERBÁKOVÁ, K., LITECKÁ, J., CSATÁRYOVÁ, M., ZAPOTOKOVÁ, M., SOLAR, V.: Research of magnetic properties of spolic technosols (alcalic/hyperartefactic) on the landfill of industrial waste from nickel production, *Journal of Electrical Engineering*, Vol. 69, No. 6, pp. 489-492, 2018. https://doi.org/10.2478/jee-2018-0083
[20] DZUBINSKA, A., FERNÁNDEZ, J.R., KUMAR, A., VARGA, R., REIFFERS, M., GIOVANNINI, M.: YOSHIZAWA, Y.: Structural and physical properties of YbCu4Ni based heavy fermion compounds, *Journal of Magnetism and Magnetic Materials*, Vol. 588, No. December, p. 171380, 2023. https://doi.org/10.1016/j.jmmm.2023.171380

Review process
Single-blind peer review process.

Acta Tecnología - International Scientific Journal about Technologies
Volume: 10 2024 Issue: 3 Pages: 99-102 ISSN 2453-675X

https://doi.org/10.22306/atec.v10i3.217 *Received: 09 July 2024; Revised: 30 Aug. 2024; Accepted: 05 Sep. 2024*

Development of a robotic wheel door opener system assistive device

Amine Mazouzi
Université Laval, Department of Mechanical Engineering, 1065 Av. de la Médecine, Québec, Canada,
amine.mazouzi.1@ulaval.ca (Corresponding author)
Simon Latour
Université Laval, Department of Mechanical Engineering, 1065 Av. de la Médecine, Québec, Canada,
simon.latour@cirris.ulaval.ca
Alexandre Campeau-Lecours
Université Laval, Department of Mechanical Engineering, 1065 Av. de la Médecine, Québec, Canada,
alexandre.campeau-lecours@gmc.ulaval.ca
Francois Routhier
Université Laval, School of Rehabilitation Sciences, 1050 Av. de la Médecine, Québec, Canada,
francois.routhier@rea.ulaval.ca

Keywords: mechatronics, assistive technology, physical disabilities, smartphone-controlled system.
Abstract: Physical disabilities significantly impact individuals' ability to perform activities of daily living (ADL), leading to reduced autonomy and difficulty to accomplish daily living tasks. One such barrier is the difficulty or inability to open doors, preventing access to different rooms in their residence (bathroom, bedroom, etc.), rooms at work, or shopping areas. Existing solutions, such as robotic arms on wheelchairs and door openers mounted at the top of doors, remain expensive, complex to install, and relatively difficult for the target population to use. Addressing this challenge, this study introduces a Robotic Wheel Door Opener System (RWDOS) designed to facilitate the opening and closing of the door. The RWDOS is installed at the bottom of a door and is controlled remotely through a smartphone application. The paper presents the mechanical design and control system along with a cost analysis. It concludes with initial results and outlines the future directions for the project.

1 Introduction

The inability to use one's arms or hands to grasp, manipulate, and move objects significantly limits an individual's ability to perform daily living tasks, work, and leisure activities. This is a common challenge for people living with physical and cognitive disabilities, which restricts their activities of daily living (ADLs) and, in turn, affects their autonomy and quality of life [1]. Moreover, a study revealed that the risk of ADL impairment increases with the number of chronic diseases in both middle-aged (45-59 years) and older adult (60-74 years) groups [2].

An example of a crucial and simple ADL task essential for daily life is opening a door. This action allows users to access different rooms in their residence (bathroom, bedroom, etc.) and enables them to go out for work, shopping, and other needs outside the home. The difficulty or inability to open a door autonomously and safely can significantly impact a person's ability to maintain their ADLs, level of autonomy, and overall quality of life.

To address this problem, home adaptations have been developed. A systematic review has shown that accessible housing has a positive physical and cognitive impact on patients' health [3]. However, in 2017, 13% of Canadians with physical disabilities indicated that they were unable to obtain the accessibility features and aids that they needed in their home [4].

2 Literature review

Existing solutions to open doors, such as assistive humanoid robots, robotic arms installed in wheelchairs [5], and automatic door openers and closers above the door [6], can be expensive, and a significant proportion of potential users are unable to afford these assistive devices. In fact, the leading reason for not obtaining the assistive device needed is cost (77% of the reasons) [7]. In addition, home installation of these assistive devices can become complicated due to several factors and, as a result, hinder the implementation of these solutions.

In the case of assistive humanoid robots, the complexity of installation and maintenance requires specialized knowledge and infrastructure, which may not be readily available in all homes. Furthermore, these robots often need significant space to operate effectively, which can be a constraint in smaller living environments. Lastly, ensuring that the robot is compatible with the unique needs and preferences of each user adds another layer of difficulty, as it often requires customization and ongoing adjustments.

As for the robotic arm on a wheelchair, the cost of these advanced assistive devices can be prohibitive, limiting their accessibility for many users. In fact, this technology is mostly used for various tasks such as pick up a drink or a phone. Moreover, the installation process can be complex, requiring modifications to both the wheelchair and the home environment, which may not always be feasible or practical. Additionally, the robotic arm needs to be finely calibrated to ensure it can operate various types of door mechanisms reliably, which can be challenging in diverse home settings. The integration of such technology with existing wheelchair systems also demands specialized maintenance and troubleshooting, which may not be readily available.

Finally, door openers installed above doors, although cheaper and less complex than the previous solutions, still require significant modifications to the existing door structure and hardware, which may not be feasible in some cases or need the intervention of a technician to install the device correctly, which will increase the costs for the user.

The originality of this article lies in its development of a robotic door opener system designed through an iterative process that closely involved occupational therapists and potential users. Specifically, the system is designed to be low-cost and easily installable on a door without requiring any modifications to the door itself. The system adapts mechanically to uneven surfaces and can be controlled via a smartphone. The system was refined through continuous feedback from actual users, ensuring that it effectively aligns with their specific needs and constraints.

3 Objective

The goal of this project is to enable people to independently move between different rooms for accessibility, autonomy, reduced need for assistance, and access to commerce and work. To achieve this goal, the objective of this study is to design a Robotic Wheel Door Opener System (RWDOS) that can be installed in users' residences and be controlled remotely. In such manner, this project will ensure accessibility for people living with upper limb disabilities. The main evaluation criteria will be manufacturing and installation cost, efficiency, along as installation simplicity.

4 Development

4.1 Mechanical design

The RWDOS design includes a motorized wheel fixed to a door, as shown in Figures 1 and 2. The 62-mm diameter wheel is attached to a two-bar mechanism that allows the wheel to move vertically, adapting to uneven floor levels during the opening or closing of the door. If the mechanism were simply a rigid bar, the wheel could lose contact with the floor at some points, or the floor could exert significant force on the assembly at other points due to its unevenness. The two-bar mechanism compensates for vertical floor height variations but cannot apply the necessary force to keep the wheel in contact with the floor. To address this, a pair of springs was added to the two-bar mechanism at the junction between the wheel support and the base. These springs, shown in Figure 1, keep the wheel in constant contact with the floor, preventing it from rolling in the air and by increasing adherence between the wheel and the floor.

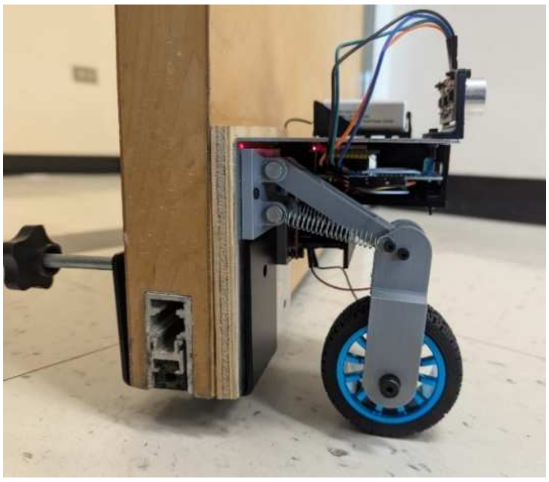

Figure 1 Side view of the WRDOS fixed on a door

The wheel is directly connected to a 25GA-370 DC motor (6V 280 rpm), responsible for its rotation movement. The DC motor, shown in Figure 2, was chosen to ensure the door can open in less than 10 seconds. The goal was to achieve an actuation time that is not too long for the user, while being slow enough for safety considerations.

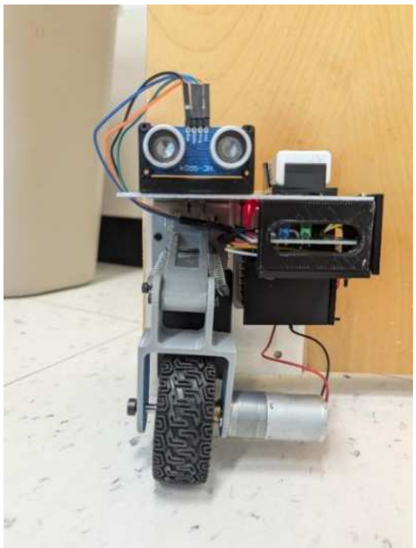

Figure 2 Front view of the wheel door opener system

4.2 Algorithm and on-board computer system

The DC motor, and consequently the door's movement, are controlled by a microcontroller (ESP32 MH-ET Minikit) through a motor driver (L298N). When the microcontroller receives the appropriate signal, it activates the DC motor to produce the desired door movement. The components are powered by a 9V battery placed at the top of the RWDOS. A functional scheme of the whole system is shown in Figure 3. The section below describes all the considerations taken to develop the RWDOS.

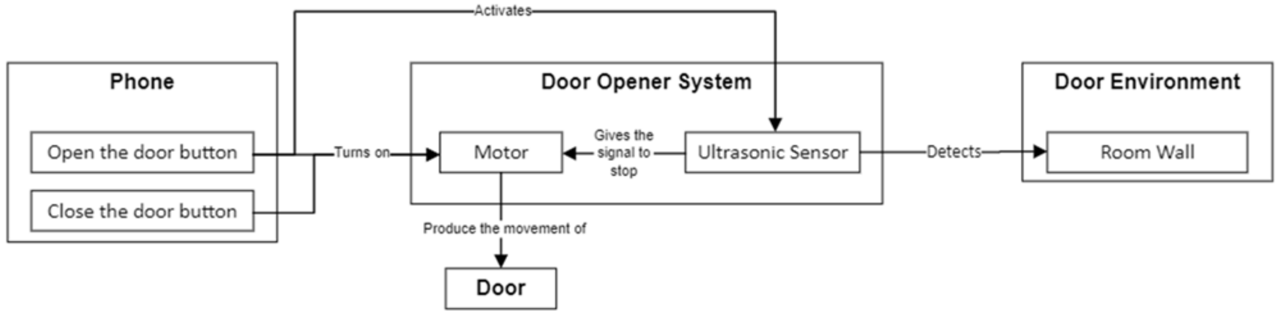

Figure 3 Functional diagram of the wheel door opener system

4.2.1 DC motor operating time

As mentioned, the DC motor must be actuated at a speed that allows efficient and safe opening/closing of the door. To this extent, a 1.5s – 7s – 1.5s speed profile (acceleration phase of 1.5s, constant speed phase of 7s and deceleration phase of 1.5s) has been chosen for the DC motor's operation. However, a challenge is that the time required to open a door can vary depending on factors such as the door's size and weight. A pre-programmed opening duration that is too short would prevent the door from opening completely, while a duration that is too long could result in a collision between the door and a wall. On the other hand, an adjustable duration might be cumbersome and less intuitive for the user.

To that end, an ultrasound sensor was installed on the front side of the RWDOS (see Figure 2). When an object, such as the wall, is detected within a predetermined range, the motor will immediately stop.

4.2.2 User interface

Many options can be used as the user interface for opening or closing the door, each with distinct advantages and drawbacks. For instance, a push button could be installed on the door, connected either via a wire or wirelessly, but this requires the patient to physically reach and press the button, which may be challenging for those with limited mobility. A classic IR remote control could be used, but this would require the user to always carry it with them and can suffer from signal loss when there is an obstruction, such as a door, between the remote and the receiver. Presence detection systems, such as cameras, although effective, are often prohibitively expensive and complex to implement. In contrast, a smartphone application, as shown in Figure 3, offers a superior solution by allowing the door to be opened from a considerable distance with ease, making it accessible for a wide range of users.

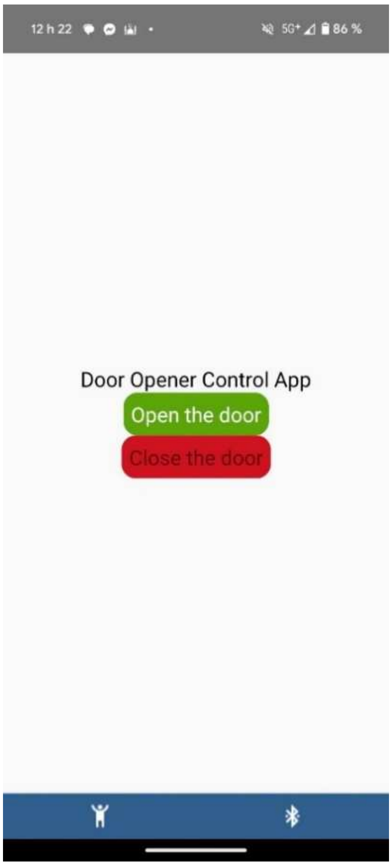

Figure 4 Wheel door opener control application

5 Discussion

In this paper, the design of a Robotic Wheel Door Opener System (RWDOS) was presented. The general objective of this project is to enable people to independently move between different rooms for accessibility, autonomy, reduced need for assistance, and access to commerce and work. At this point, the RWDOS can open and close a standard door in less than 10 seconds successfully. Additionally, the response time to the order sent by the smartphone application is almost instantaneous. The ultrasound sensor allowed a quick reaction of the system in case of room wall detection, stopping the motor before any physical contact. Finally, the cost of the first prototype has been evaluated at 300 CAD as shown in

Table 1. Nevertheless, this cost analysis was based on the production of approximately ten prototypes using prototyping components. If the project reaches the stage of manufacturing for personal use, fabrication processes and product design will be reviewed to reduce the cost and make the product more accessible.

Table 1 Cost analysis of the project.

Parts/components	75 $
Raw materials	25 $
Manufacturing Processes	110 $
Other costs (maintenance charges, training for users, etc.)	40 $
Subtotal	250 $
Unforeseen (as a percentage added to the subtotal)	20%
Total	**300 $**

6 Conclusion

The future of this project will primarily involve validating the device with rehabilitation professionals and end-users. In other words, the device will be tested in household environments with the involvement of rehabilitation professionals to evaluate its practical usability and impact on daily rehabilitation activities. Indeed, gathering feedback from real users will be essential for evaluating the system's efficiency and user satisfaction, thereby informing iterative design improvements. Based on the results and feedback received, the system will be enhanced. Additionally, technical improvements will be made to the device, focusing on sourcing parts to reduce costs and redesigning elements for cost efficiency. Through these efforts, we aim to refine the robotic assistant system to better meet the needs of therapists and patients, ultimately contributing to a higher quality of care and increased independence for users.

Acknowledgement
This project was supported by the Centre for Interdisciplinary Research in Rehabilitation and Social Integration (Cirris) and the Fonds de recherche du Québec – Santé (FRQS) # 251649 and # 296761.

References

[1] Gouvernement du Québec, Understanding the causes and recognizing the signs of loss of autonomy in seniors, [Online], Available: https://juridiqc.gouv.qc.ca/en/seniors-experiencing-a-loss-of-autonomy/understanding-and-planning-for-a-loss-of-autonomy/assessing-and-preserving-your-autonomy/understanding-the-causes-and-recognizing-the-signs-of-loss-of-autonomy-in-seniors, [21 Jun 2024], 2024.
[2] AI, Z., TANG, C., WEN, X., KARTHEEPAN, K., TANG, S.: Examining the impact of chronic diseases on activities of daily living of middle-aged and older adults aged 45 years and above in China: A nationally representative cohort study, *Frontiers in Public Health*, Vol. 11, pp. 1-10, 2024. https://doi.org/10.3389/fpubh.2023.1303137
[3] CHO, H.Y., MACLACHLAN, M., CLARKE, M., MANNAN, H.: Accessible home environments for people with functional limitations: A systematic review, *International Journal of Environmental Research and Public Health*, Vol., 13, No. 8, 826, pp. 1-24, 2016. https://doi.org/10.3390/ijerph13080826
[4] GAMEY, J.: What is 'accessible housing' and why does Canada need more of it?, PEACH Research Unit, [Online], Available: https://peachresearch.ca/what-is-accessible-housing-and-why-does-canada-need-more-of-it/#:~:text=Of%20the%2055.8%25%20of%20Canadians,increasingly%20urgent%20issue%20in%20Canada [21 Jun 2024], 2023.
[5] VOGEL, J., LEIDNER, D., HAGENGRUBER, A., PANZIRSCH, M., BÄUML, B., DENNINGER, M., HILLENBRAND, U., SUCHENWIRTH, L., SCHMAUS, P., SEWTZ, M., BAUER, A., HULIN, T., ISKANDAR, M., QUERE, G., ALBU-SCHÄFFER, A., DIETRICH, A.: An Ecosystem for Heterogeneous Robotic Assistants in Caregiving, Core functionalities and use cases, *IEEE Robotics & Automation Magazine*, Vol. 28, No. 3, pp. 12-28, 2021. https://doi.org/10.1109/MRA.2020.3032142
[6] SURAVASE, V., SHINDE, V., SHIRSAT, D., DIWATE, S.S., PALHE, S.N.: Automation of Door Opening & Closing, *TechRxiv*, Vol. 2021, pp. 1-6, 2021. https://doi.org/10.36227/techrxiv.14724801.v1
[7] Statistics Canada, Needs for mobility devices, home modifications and personal assistance among Canadians with disabilities, [Online], Available: https://www150.statcan.gc.ca/n1/pub/82-003-x/2017008/article/54852-eng.htm [21 Jun 2024], 2017.

Review process
Single-blind peer review process.

Acta Tecnología – International Scientific Journal about Technologies
Volume: 10 2024 Issue: 3 Pages: 103-107 ISSN 2453-675X

https://doi.org/10.22306/atec.v10i3.221 *Received: 13 Aug. 2024; Revised: 27 Aug. 2024; Accepted: 18 Sep. 2024*

Prototype design and analysis of a mobile robot

Dang Anh Viet
VNU University of Engineering and Technology, 144 Xuan Thuy Street, Cau Giay District, Ha Noi, Vietnam,
vietda@vnu.edu.vn

Keywords: mobile robot, design, robot arm.
Abstract: Mobile robots are robots that can move on their own. Robots move in their environment, not fixed to a real location. With the flexibility of the navigation wheel combined with the dynamic system, the wheeled mobile robot is suitable for flexible movement on flat terrain, using tank-like tracks will be suitable for moving on difficult, complex, bumpy terrain. The article introduces a process of developing, designing a mobile robot combining a 4-degree-of-freedom arm with a mobile chassis. Kinematics, dynamics, strength of structure testing and simulation are all calculated in detail. Finally, a prototype was built and tested to prove the correctness of the process. The project has calculated the kinematics and dynamics of the model, thereby building trajectories, designing controllers for the vehicle and manipulator, thereby simulating problems on Matlab-Simulink. Designing 3D CAD models, building hardware, and testing CAE durability on Abaqus software. The results are visually tested by software, with high feasibility, is the premise for manufacturing.

1 Introduction

Industrial robots are robots designed to work in industrial production environments. Robots have been and are an indispensable part of production. Robots help increase productivity, save space, reduce labor costs, improve quality and labor safety [1-6].

Mobile robots are robots that can move on their own. Robots move in their environment, not fixed to a real location [7-9]. Mobile robots are different from industrial robots that are usually placed near fixed and operate with arms, mobile robots are capable of performing tasks in many different locations instead of being fixed in one place like other types of robots. With the flexibility of the navigation wheel combined with the dynamic system, the wheeled mobile robot is suitable for flexible movement on flat terrain, using tank-like tracks will be suitable for moving on difficult, complex, bumpy terrain.

Currently, the world has been developing mobile arm robot lines to perform many different tasks such as: flexible navigation and automatic movement of the robot to the required place accurately and safely or automatic navigation of parts. The most common type of robot arm that performs the function of picking and placing objects in industrial production[10-14]. This robot arm will pick up objects from one position and drop them at another position. The farther the distance between these two positions, the larger the requirement for the arm size, leading to high manufacturing costs. Therefore, combining a mobile cart with a pick and place robot arm is an ideal combination, increasing the working space of the robot arm.

The article introduces a process of developing, designing and manufacturing a mobile robot combining a 4-degree-of-freedom arm with a mobile chassis. Kinematics, dynamics, strength of structure testing and simulation are all calculated in detail. Finally, a prototype was built and tested to prove the correctness of the process.

2 Methodology

2.1 Kinetic of wheel mobile

Figure 1 shows the basic structure of a mobile robot, consisting of two main parts: a mobile vehicle combined with a 4-degree-of-freedom robot arm. Mobile robot kinematics is the most basic problem of how a robot system works.

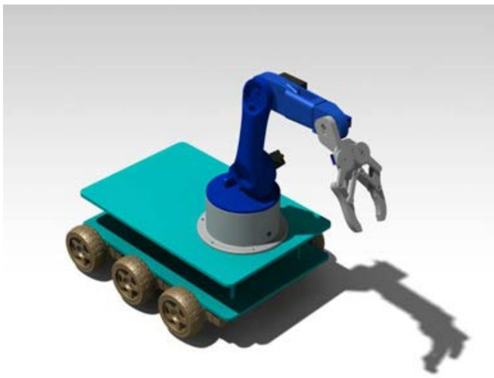

Figure1 Mobile robot CAD modelling

The kinematic equations will give the relationships between the control parameters and build the robot's state in space, the way the robot moves without considering the impact force (1).

$$v = \frac{(v_r + v_l)}{2} \ and \ \omega = \frac{(v_r - v_l)}{L} \quad (1)$$

In which:
v_l– velocity of the left wheel,
v_r – velocity of the right wheel,
L – distance between the 2 wheels,
R – Wheel radius.

From there the instantaneous radius of curvature of the trajectory is calculated by the equation (2):

$$R = \frac{L.(v_r + v_l)}{2.(v_r - v_l)} \quad (2)$$

2.2 Mobile trajectory simulation

The motion trajectory is described as in Figure 2, including 2 straight motions and 1 curved motion.

Figure 2 Mobile robot trajectory

Time motion on a half of circle (3), (4):

$$t = \frac{s}{v} = \frac{\pi.R}{(v_r+v_l)/2} = \frac{0.225.\pi}{(0.1+0.05)/2} = 9.43s \quad (3)$$

Time on straight line $t = \frac{0.5}{(v_r+v_l)/2} = 10s$ (4)

Conduct orbital movement model creation and simulation, the results obtained are as described in Figure 3, the results are consistent with the calculation.

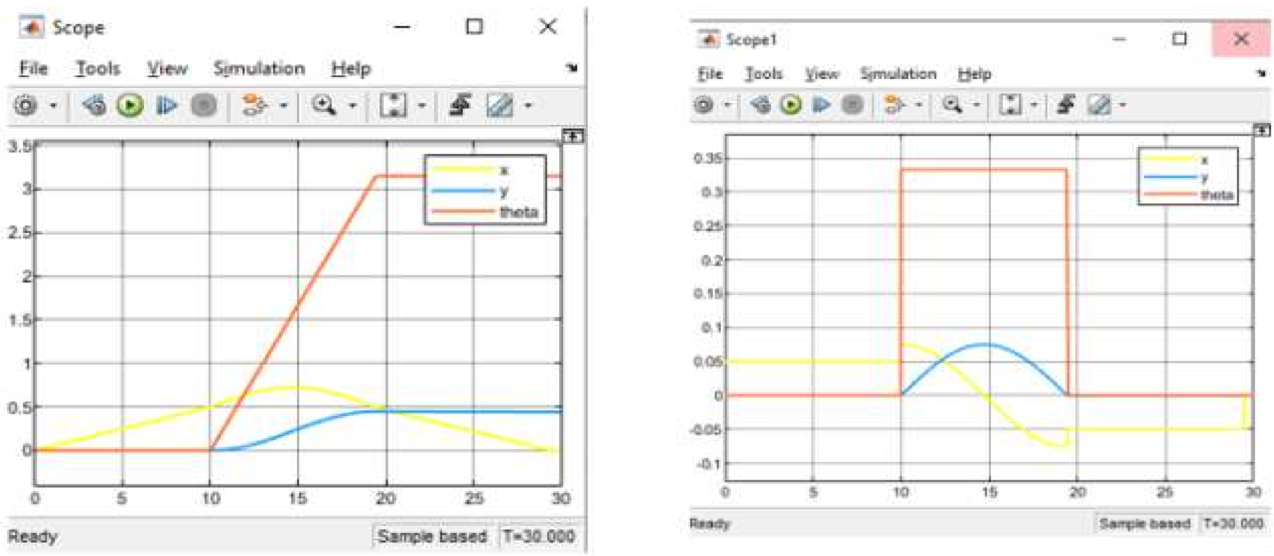

Figure 3 Velocity simulation

After calculating the velocity problems, the robot's motion trajectory is calculated as shown in Figure 4. The motion trajectories in the X, Y and angle directions are all calculated, with the aim of providing the robot's working space.

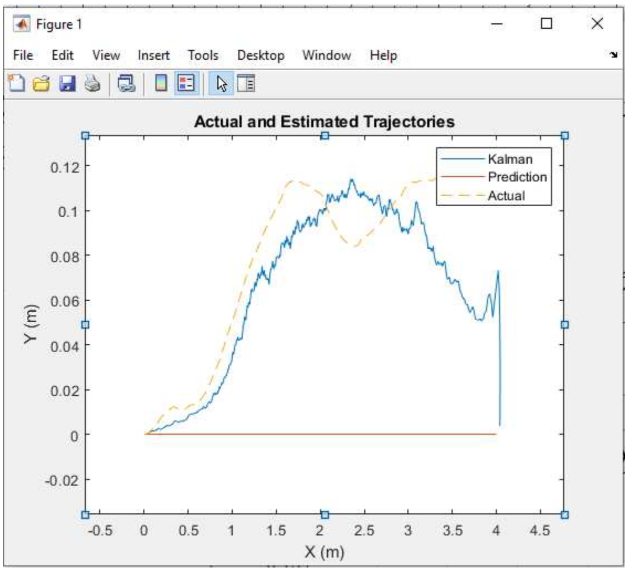

Figure 4 Investigating robot trajectory through simulation

2.3 Robot arm modelling

Figure 5 shows the 4-degree-of-freedom robot arm mounted on the chassis. The arm's kinematics, dynamics and workspace are shown in Figure 6, Figure 7, Figure 8 and Figure 9. The reversible, velocity and position problems are all considered in detail.

Figure 5 Robot arm CAD model

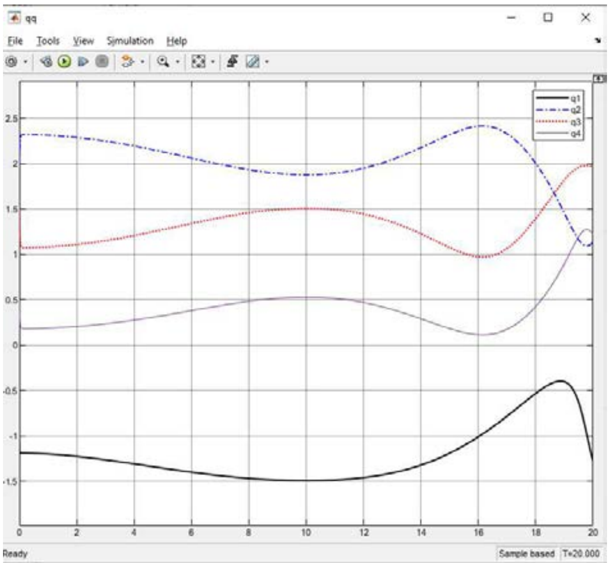

Figure 6 DH parameter values

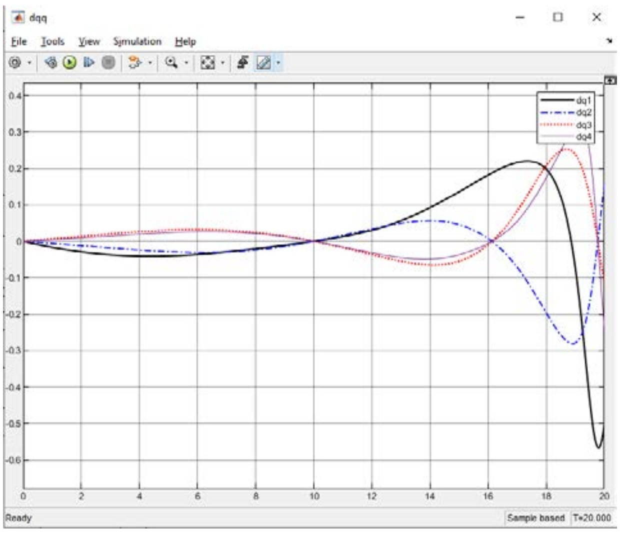

Figure 7 The velocity value diagram process

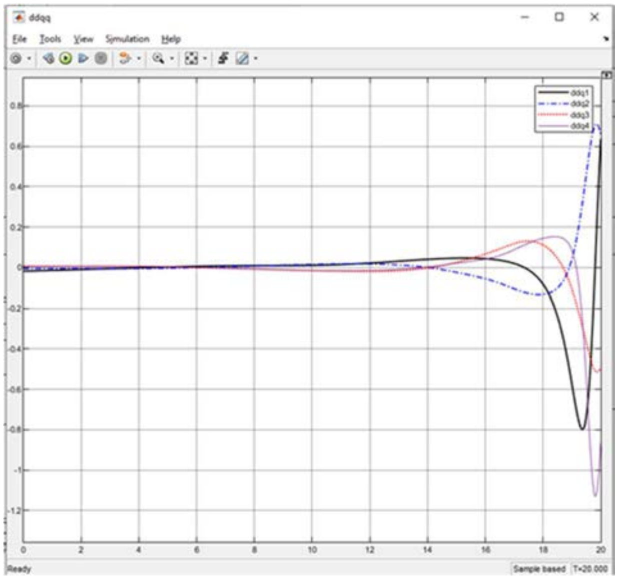

Figure 8 The acceleration value diagram process

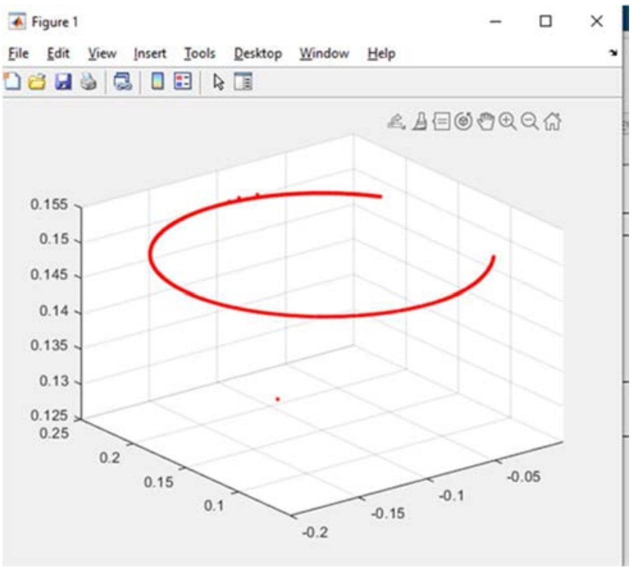

Figure 9 Robot trajectory in the workspace

The robot arm model is 75 cm high, 30 cm long and 25 cm wide, with a total mass of 3 kg. The robot is capable of picking up objects weighing 200 g.

2.4 Strength of structure testing

Strength testing is a necessary step to ensure the system works stably before it can be manufactured, this is an important step in any design of any machine.

Figure 10 shows that the shear stress on the wheel motor is mainly concentrated at the end of the motor and the end of the wheel joint attached to the motor. The stress is in the range from 400Pa to 700Pa. As for the frame, the shear stress is mainly concentrated at the lower layer of the frame and the end of the lower connecting rod is subjected to the highest pressure in the range of 700 to 1000 Pa.

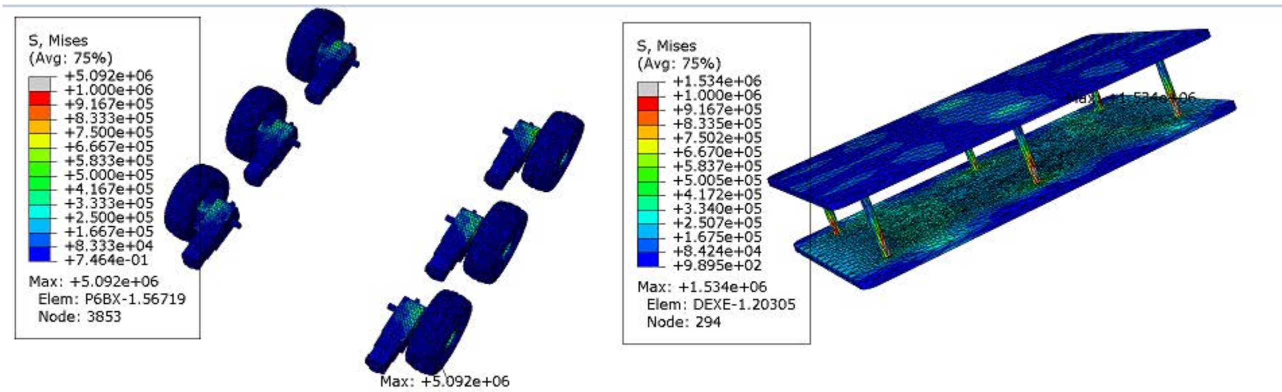

Figure 10 Tensile stress simulation on wheel and frame

Figure 11 shows that the normal stress on the wheel motor is concentrated mostly at the wheel-motor connection area in the range of 60Pa to 200 Pa. As for the frame, it is mainly concentrated on the bottom surface and at the contact part of the connecting rod in the range of 200Pa to 500Pa.

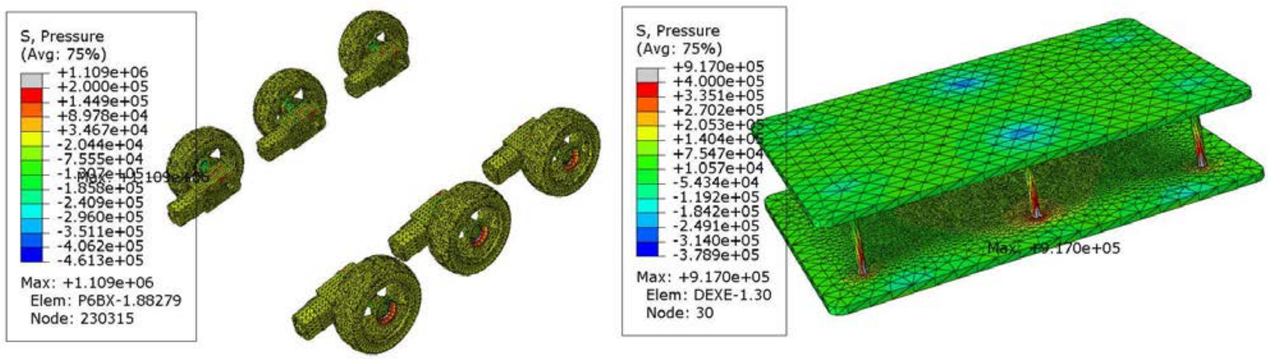

Figure 11 Shear stress simulation on wheel and frame

Figure 12 shows that the displacement at the engine wheel and the chassis increases from the inside out. The maximum value is reached at the end with the displacement value. As for the chassis, the maximum displacement value reaches 1.28cm at the two ends of the chassis. From the durability tests for the chassis structure, it is found that the chassis structure is completely strength enough to ensure working capacity.

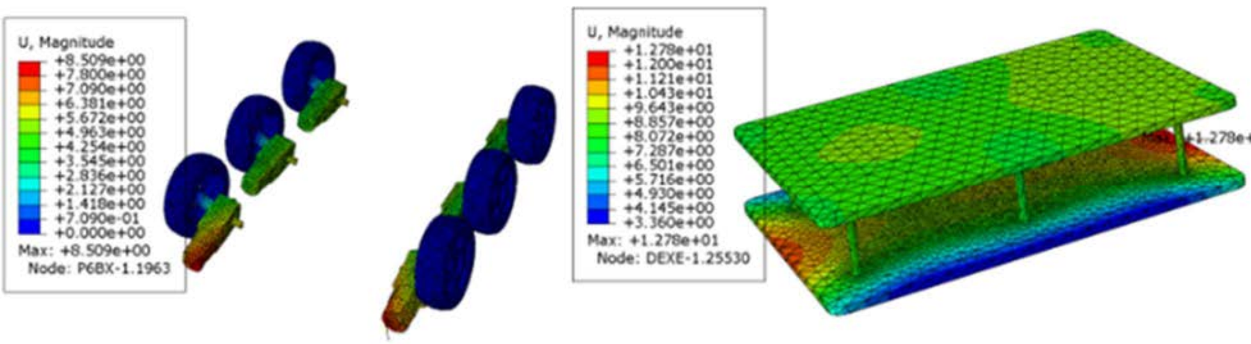

Figure 12 Displacement higher on wheel and frame

3 Result and discussion

Figure 13 shows an overview of the proposed mobile robot model. Capable of picking up objects up to 0.4 kg, the vehicle is capable of moving straight and at an angle. Overall assessment of the model is complete and meets the criteria for a mobile robot model combining a four-link manipulator capable of recognizing objects. However, the accuracy and operating time can be further improved to help the model become more complete.

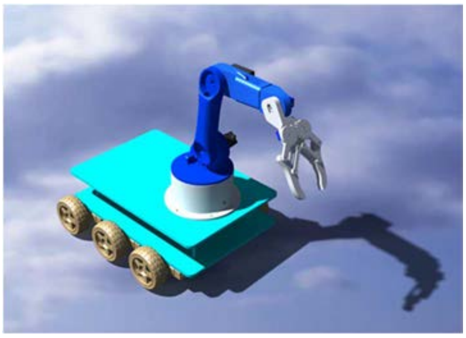

Figure 13 Mobile robot construction

4 Conclusions

The article proposed a research process to build and implement a mobile robot combined with a 4-degree-of-freedom manipulator. Capable of picking up objects up to 0.4 kg, the vehicle is capable of moving straight and at an angle., The time to perform a pick and place cycle is about 50 seconds. The project has calculated the kinematics and dynamics of the model, thereby building trajectories, designing controllers for the vehicle and manipulator, thereby simulating problems on Matlab-Simulink. Designing 3D CAD models, building hardware, and testing CAE durability on Abaqus software. A mobile robot prototype has been designed and developed. The mechanical components have been presented. Dynamic analyses have been performed to model the system operation. The developed prototype has proven to be reliable and stable and can be manufactured in future works. The results are visually tested by software, with high feasibility, is the premise for manufacturing.

References

[1] KE, X., YU, Y., LI, K., WANG, T., ZHONG, B., WANG, Z., KONG, L., GUO, J., HUANG, L., IDIR, M., LIU, C., WANG, C.: Review on robot-assisted polishing: Status and future trends, *Robotics and Computer-Integrated Manufacturing*, Vol. 80, No. April, pp. 1-28, 2023. https://doi.org/10.1016/j.rcim.2022.102482

[2] ZHENG, C., QIN, X., EYNARD, B., BAI, J., LI, J., ZHANG, Y.: SME-oriented flexible design approach for robotic manufacturing systems, *Journal of Manufacturing Systems*, Vol. 53, No. October, pp. 62-74, 2019. https://doi.org/10.1016/j.jmsy.2019.09.010

[3] VAISI, B.: A review of optimization models and applications in robotic manufacturing systems, Industry 4.0 and beyond, *Decision Analytics Journal*, Vol. 2, No. March, pp. 1-18, 2022. https://doi.org/10.1016/j.dajour.2022.100031

[4] RIBEIRO, J., LIMA, R., ECKHARDT, T., PAIVA, S.: Robotic Process Automation and Artificial Intelligence in Industry 4.0 – A Literature review, *Procedia Computer Science*, Vol. 181, pp. 51-58, 2021. https://doi.org/10.1016/j.procs.2021.01.104

[5] JAVAID, M., HALEEM, A., SINGH, R.P., SUMAN, R.: Substantial capabilities of robotics in enhancing industry 4.0 implementation, *Cognitive Robotics*, Vol. 1, pp. 58-75, 2021. https://doi.org/10.1016/j.cogr.2021.06.001

[6] TUNG, T.T., QUYNH, N.X., MINH, T.V.: A prototype of auto badminton training robot, *Results in Engineering*, Vol. 13, No. March, 100344, pp. 1-6, 2022. https://doi.org/10.1016/j.rineng.2022.100344

[7] RAJ, R., KOS, A.: A Comprehensive Study of Mobile Robot: History, Developments, Applications, and Future Research Perspectives, Applied Sciences, Vol. 12, No. 14, 6951, pp. 1-26, 2022. https://doi.org/10.3390/app12146951

[8] LOGANATHAN, A., AHMAD, N.S.: A systematic review on recent advances in autonomous mobile robot navigation, *Engineering Science and Technology, an International Journal*, Vol. 40, No. April, 101343, pp. 1-26, 2023. https://doi.org/10.1016/j.jestch.2023.101343

[9] RUBIO, F., VALERO, F., LLOPIS-ALBERT, C.: A review of mobile robots: Concepts, methods, theoretical framework, and applications, *International Journal of Advanced Robotic Systems*, Vol. 16, No. 2, 2019. https://doi.org/10.1177/1729881419839596

[10] TUNG, T.T., ANH, N.H., MINH, T.V.: *Design and Structure Analysis of a Prototype Industrial Robot Arm*, ICRSA '23: Proceedings of the 2023 6th International Conference on Robot Systems and Applications, pp. 81-85, 2023. https://doi.org/10.1145/3655532.3655545

[11] LI, K., HUO, Y., LIU, Y., SHI, Y., HE, Z., CUI, Y.: Design of a lightweight robotic arm for kiwifruit pollination, *Computers and Electronics in Agriculture*, Vol. 198, No. July, pp. 1-18, 2022. https://doi.org/10.1016/j.compag.2022.107114

[12] ZHANG, C., LI, S., ZHANG, Z.: Industrial robot arm dynamic modeling simulation and variable-gain iterative learning control strategy design, *Journal of Mechanical Science and Technology*, Vol. 38, pp. 3729-3739, 2024. https://doi.org/10.1007/s12206-024-0644-5

[13] TUNG, T.T., TINH, N.V., THAO, D.T.P., MINH, T.V.: Development of a prototype 6 degree of freedom robot arm, *Results in Engineering*, Vol. 18, No. June, 101049, pp. 1-12, 2023. https://doi.org/10.1016/j.rineng.2023.101049

[14] YU, C., LI, Z., YANG, D., LIU, H.: A fast robotic arm gravity compensation updating approach for industrial application using sparse selection and reconstruction, *Robotics and Autonomous Systems*, Vol. 149, No. March, pp. 1-15, 2022. https://doi.org/10.1016/j.robot.2021.103971

Review process
Single-blind peer review process.

JOURNAL STATEMENT

Journal name:	**Acta Tecnología**
Abbreviated key title:	Acta Tecnol
Journal title initials:	AT
Journal doi:	10.22306/atec
ISSN:	2453-675X
Start year:	2015
The first publishing:	October 2015
Issue publishing:	Quarterly
Publishing form:	On-line electronic publishing
Availability of articles:	Open Access Journal
Journal license:	CC BY-NC
Publication ethics:	COPE, ELSEVIER Publishing Ethics
Plagiarism check:	Worldwide originality control system
Peer review process:	Single-blind review at least two reviewers
Language:	English
Journal e-mail:	**info@actatecnologia.eu**

The journal focuses mainly on the original and new, interesting, high-quality, theoretical, practical and application-oriented contributions to science and research and pedagogy and education in technologies.

Acta Tecnologia journal supports the San Francisco Declaration on Research Assessment (DORA). The primary directives include open access, reuse of outputs, diversity among authors and reviewers, peer review, description of provided services and related publishing charges.

Publisher:	**4S go, s.r.o.**
Address:	Semsa 24, 044 21 Semsa, Slovak Republic, EU
Phone:	+421 948 366 110
Publisher e-mail:	**info@4sgo.eu**

Responsibility for the content of a manuscript rests upon the authors and not upon the editors or the publisher.